UiT The Arctic University of Norway

Faculty of Science and Technology
Department of Physics and Technology

Introducing Glycemic Index to Blood Glucose Simulations and its effect on Food Recommendation Systems

Håvard Strid Buholdt

FYS-3941 Master's Thesis in Applied Physics and Mathematics 30 SP - December 2024

Abstract

The availability of In-Silco blood glucose simulators that accurately depict all aspects of Diabetes Mellitus patient's daily life is crucial for the development of safe and effective new treatment technologies. Current state of the art simulators focus on modeling a meal's effect on the glucose-insulin system solely based on the quantity of carbohydrates consumed. However not only the quantity of carbohydrates consumed effects the glycemic response, but also the quality of these consumed carbohydrates.

Regular exercise is an important factor in the treatment of diabetes as it yields many benefits for the patient's health. However, states of hypoglycemia are common during physical activities which may cause patients to avoid exercising.

This thesis proposes an extension to the currant state of the art blood glucose simulator that introduces food's glycemic index and its effect on the glucose-insulin system. This extension is then used to develop food recommendation systems for type-1 diabetes patients, to recommend the optimal food to keep the blood glucose concentrations in the normoglycemic range during exercise sessions. And a experiment is conducted to determine how knowing food's glycemic index affects these systems.

The simulations of the proposed extension is shown to correctly capture the effect a food's glycemic index has on the postprandial blood glucose response as described in literature. And the result of the experiment depict a positive impact of using glycemic index knowledge in food recommendation systems that grows as the length and intensity of the exercise sessions increases.

Acknowledgements

I would like to thank my supervisors;
Phuong Dinh Ngo, Miguel Tejedor Hernandez and Fred Godtliebsen,
for productive feedback and good discussions on our weekly meetings.

I would also like to thank my family for always supporting me, and a special thanks goes out to my dear Hannah.

Contents

List of Figures

List of Tables

List of Abbreviations

AI Artificial Intelligence

APMHR Age-Predicted Maximum Heart Rate

BG Blood Glucose

BW Body Weight

CGM Continuous Glucose Monitor

CHO Carbohydrate

FDA The United States Food and Drug Administration

FFNN Feed Forward Neural Network

GI Glycemic Index

GL Glycemic Load

HR Heart Rate

MSE Mean Squerd Error

NN Neural Network

PA Physical Activity

RL Reinforcement Learning

T1DDS Type-1 Diabetes Direct Simulator

T1DM Type-1 Diabetes Mellitus

T2DM Type-2 Diabetes Mellitus

TIR Time In Range

UVA University of Virginia

1 Introduction

The availability of In-Silco Blood Glucose (BG) simulators that accurately depict all aspects of Type-1 Diabetes Mellitus (T1DM) patient's daily life is crucial for the development of safe and effective new diabetes treatment technologies like artificial pancreas systems, food recommendation systems, and other mobile health systems [1]. Current state of the art BG simulators focus on modeling a meal's effect on the glucose-insulin system solely based on the quantity of carbohydrates in the meal. However, not only the quantity of consumed carbohydrates effects the following glycemic response, but also the quality of these consumed carbohydrates. Consumption of a meal rich in high Glycemic Index (GI) carbohydrates will generally produce a quicker spike in postprandial BG concentration with higher amplitude than a meal containing the same amount of low GI carbohydrates.

This thesis proposes an extension to the UVA/Padova BG simulator that implements the effect a food's GI has on the glucose-insulin system and looks at how this extension can be used in the development of food recommendation systems. Describing meals in terms of both carbohydrates and GI allows for a more nuanced and realistic postprandial BG simulations, better suited to depict the BG dynamics of patients daily life.

One area of interest for an extension like this is the development of food recommendation systems. Mobile health systems like these usually require immense amounts of data, and collecting enough in-vivo data to train these systems is often challenging, expensive, impractical and time-consuming. In-

Silco simulations are therefor a good alternative for data collecting.

Regular exercise is an important factor in the treatment of diabetes as it yields many benefits for the patient's health and is associated with lowering the BG concentrations [2]. However, many patients experience states of hypoglycemia during exercises due to this lowering effect. As hypoglycemic unawareness is common in patients with diabetes, these states might go undetected and lead to more severe consequences [3]. This may be unpleasant for patients and might cause them to develop restraints toward physical activities due to fear of hypoglycemia.

A food recommendation system is supposed to recommend the optimal food to keep the patient's BG concentrations in the normoglycemic range and avoid states of hypoglycemia. The availability of an effective food recommendation system might be able ease this restraint towards physical activity by decreasing the risk of experiencing hypoglycemia under exercise and allowing for healthier exercise sessions.

1.1 Related work

To the knowledge of the author, prior studies/work on integrating GI to BG simulators do not exist. Noguchi et al. (2016) [4] utilized a technique where a food's GI is depicted by scaling the carbohydrate amount of the simulated foods. However, this will not depict the full BG response associated with different GI foods as the simulated response will only be scaled and not changed in length or shape.

Prior work exists, however, on food recommendation systems and how these can be utilized for scenarios of physical activity in T1DM patients. The following paragraphs will depict two of the studies that inspired the food recommendation system developed in this thesis.

Ngo et al. (2019) [2] developed food recommendation systems from in-silco T1DM patient data of the Hovorka simulation model [5], with the goal of controlling the virtual patient's BG concentration during short and long scenarios of physical activities. Foods for the short scenarios where recommended by a Feed Forward Neural Network (FFNN) trained to predict the optimal amount of carbohydrates to consume before the sessions while for the longer session, a Reinforcement Learning (RL) agent was trained to recommend the optimal amount of carbohydrates to consume at fixed intervals through the scenarios, thereby proving that machine learning could be used to develop patient-specific food recommendations systems for exercise scenarios [2].

In a later study; Ngo et al. (2020) [6] combined the FFNN based food recommendation system earlier developed with a Bayesian FFNN to accurately depict the BG response as well as the risk of hyperglycemia and hypoglycemia of each recommendation. These systems where trained on the in-silco data from the UVA/Padova simulator using Bretons Physical Activity (PA) extension[7; 1]. The results of the study depicted a safer and effective management of the BG concentrations both during and post exercise scenarios [6].

1.2 Outline

This thesis is comprised of four parts. Part I, will introduce the necessary background needed for the thesis. This includes theory on topics such as Diabetes Mellitus, Glycemic Index, state of the art Blood Glucose simulators and artificial Neural Network. Chapter 2 present both Type-1 Diabetes Mellitus (T1DM) and Type-2 Diabetes Mellitus (T2DM), and how these diseases effect the glucose-insulin dynamics as well as some state of the art diabetes treatment strategies. Chapter 3 present the Glycemic Index, what it represents, how it is defined and how it can be calculated. In chapter **??**, we presents state of the art BG simulation models like the UVA/Padova model [7] as well as existing extensions to the model, adding the effect physical activities has on the glucose-insulin system. This chapter will also include a detailed depiction of the digestion and oral glucose absorption in the model which will be important to the proposed GI extension. The final chapter of part I, will present the fundamentals of Feed Forward Neural Networks.

Part II presents our proposed GI extension. This includes the methodology, result and discussion of the proposed extension. The methodology of the extension is presented in chapter 6, describing how GI and its effect on the glucose-insulin system were implemented into the simulation model. Chapter 7 presents the modeling results and illustrates postprandial BG simulations of the extended simulation model. A detailed discussion of the extensions results and methodology will follow in chapter 8.

Part III will present how the proposed extension of part II, can be used to develop food recommendation systems. This part will follow a structure similar to that of part II, including both methodology, results and discussions. The methodology of the food recommendation systems is presented in chapter 9. Here, both the architecture and data of the systems will be described. Chapter 10 present the experiment conducted to determine the impact knowing food GI has on food recommendation systems. The results of this experiment will be presented in chapter 11, and discussed in chapter 12.

The final part, part IV, will recapitulate the results and finding of the thesis.

Part I

Background

2

Diabetes Mellitus

Diabetes Mellitus is a chronic metabolic disease characterized by increased Blood Glucose (BG) levels [8]. It is caused by the body either producing to little insulin or being unable to effectively use the insulin it produces [9]. Insulin is the body's main defense against rising BG levels, allowing glucose to be absorbed into the cells. Diabetes Mellitus patients have a deficiency in the systems related to the production or utilization of insulin that leads to chronically high BG levels. Repeated exposure to states of high BG levels may cause long term damage to organs such as the brain, heart, kidneys, and more, and may even lead to complete organ failure [10].

Diabetes Mellitus can present itself in three different forms: Type-1 Diabetes Mellitus (T1DM), an autoimmune disease where the body's immune system attacks the islet beta cells in the pancreas responsible for insulin production[11], causing the pancreas to produce little to no insulin [12]; Type-2 Diabetes Mellitus (T2DM), a common disease which occurs when the body develops resistance to insulin or when the pancreas produces less insulin than needed [11; 9]; and Gestational Diabetes, a form of diabetes that only occurs during pregnancy causing increased BG levels for both the mother and the baby [13]. While genetics plays a role in all three types of diabetes, the insulin resistance that causes T2DM has been shown to be related to excessive body fat, and is most common among adults over the age of 45 [11]. Gestational Diabetes is sometimes shown to be related to the hormonal changes undergone due to pregnancy, decreasing the body's ability to utilize insulin effectively [13].

2.1 Glucose-Insulin Dynamics

To ensure normal body function it is crucial to keep BG levels in the normoglycemic range of $[70, 180]$mg/dL at all times [9; 14; 6]. Both too high BG levels, hyperglycemia, and too low BG levels, hypoglycemia, can be harmful to the human body. The hyperglycemic states, defined by BG values over 180mg/dL, are a chronic condition of diabetes that can cause harm to a wide range of organs and essential systems in the human body, which may lead to organ failure. The hypoglycemic states on the other hand, defined by BG values less then 70mg/dL, is an acute condition of diabetes which causes symptoms ranging from increased heart rate to mental confusion and unconsciousness, and can cause brain damage if often repeated [2].

In the human body, two hormones are responsible for regulating the BG levels, insulin, the hormone responsible for reducing BG levels, and glucagon, the hormone responsible for increasing the BG levels. Insulin effects the BG by stimulating the cells to absorb glucose from the plasma, thereby lowering BG values. Glucagon on the other hand stimulates the liver to release stored glucose into the plasma, thereby increasing BG values. Both insulin and glucagon are only produced in the pancreas. Glucagon is secreted by the alpha cells found in the islet tissue of the pancreas, and insulin is secreted by the beta cells also found in the islet tissue of the pancreas. The production of these hormones is regulated by the amount of glucose circulating the plasma [15]. If there is too much glucose circulating the plasma, the pancreas will increase insulin secretion and inhibit glucagon secretion. Conversely, if there is too little glucose circulating the plasma, the pancreas will increase glucagon secretion and reduce insulin secretion to the basal level [16]. This balance of opposing insulin and glucagon actions is known as "Glucose homeostasis" [9].

2.1.1 The effect of Meals and Physical Activity

Several factors may effect the glucose homeostasis, ranging from metabolic disorders such as diabetes to simple things like meals and exercise. The primary way glucose is introduced to the human body is through carbohydrate rich meals. During digestion, carbohydrates (comprised of more complex sugars) are broken down to monosaccharides (simple sugars). These monosaccharides are then absorbed into the plasma resulting in rising BG levels [17]. In contrast, exercise through physical activity is thought to have an lowering effect on the BG concentration by increasing the uptake of glucose by muscle cells [18; 2].

2.2 State-of-the-art Diabetes treatment

Although there is no current cure for diabetes, treatment strategies to lessen the effect of the disease have been around for quite some time now. These strategies revolve around controlling the patients' BG to avoid hyperglycemia, usually through a combination of strict diet, regular exercise and external insulin infusions. Both diet and exercises are shown to be important factors in the treatment of diabetes. However, the most important factor is still considered to be insulin infusions, especially for T1DM [19]. The body of a T1DM patient does not produce enough insulin to successfully control the BG concentration by it self, and is therefor dependent on insulin infusions form external sources to do so.

Insulin therapy is the treatment of diabetes through the use of external insulin infusions. For the therapy to be successful, multiple measurements of the patient's BG levels must be conducted throughout the day, the amount of carbohydrates consumed by the patient needs to be counted, and insulin doses must be administrated respectively to these measurements and accounts [9].

The treatment of diabetes is considered to be a labor intensive tasks as it is a continuous process and needs to be done every day to reduce the risk of further complications. Because of this, treatment strategies rely heavily on the patient ability to self-treat. BG measuring, CHO counting and administrating insulin injections are only some of the required tasks T1DM patients need to do on a daily basis. To aid the treatment, a patient's specific treatment plan is usually designed with the help of a physician. However, the patients themselves are still responsible for following this plan [9].

The dependence on self-treatment is a downside of diabetes treatment, not only because of the amount of work needed to be done by each patient, but more because patients, as all human beings, are prone to making errors. An error in the BG measurements or the CHO counting can result in the administrated insulin dose being too small or too large. If the injected insulin dose is too small then the risk of hyperglycemia increases, and similarly, if the injected dose is too large, the risk of hypoglycemia increases. Errors like this can be counteracted if the mistake is detected in a reasonably time frame by either administrating a correction dose of insulin or consuming food rich in fast acting carbohydrates, but if the mistake goes undetected it can potentially cause harm. Mistakes that result in too much insulin being administrated are especially dangerous as insulin overdoses can lead to sever hypoglycemia and may be fatal [20]. Additionally, many diabetic patients develop insensitivities to symptoms of early stage hypoglycemia, making it harder for them to detect the hypoglycemic state. And some might not experience any symptoms

at all before approaching dangerously low BG levels. This phenomenon is called *hypoglycemic unawareness* and contributes to the increased risk of severe hypoglycemia in T1DM patients [3; 2].

2.2.1 The Basal-bolus insulin regime

One of the traditionally common treatment strategies in insulin therapy is the *Basal-bolus insulin regime*. This strategies revolves around using a combination of long acting basal insulin infusions and short acting bolus insulin infusions to mimic normal insulin production [21]. The long acting basal insulin is used to combat rising BG in states of fasting, mimicking the effect of the basal/base rate of insulin secreted by a healthy pancreas at all time. The short acting bolus insulin is used to combat rising BG levels caused by the consumption of food, thereby mimicking the increase in insulin secretion seen at meal times in healthy pancreas. Doses of basal insulin are commonly taken once or twice a day, while bolus insulin doses are taken in advance of meals to account for the time it takes for the dose to start having an effect. The size of the bolus dose depends on the meal, the more carbohydrates there are in the following meal, the bigger the basal dose needs to be to counteract it.

2.2.2 Continuous Glucose Monitor

Treatment strategies such as the basal-bolus insulin regime are dependent on regular measurements of the patients BG levels to work successfully. These measurements are traditionally done by piercing a patients fingertip to produce a blood sample to measure the glucose concentration of. The need for piercing ones fingertip is often seen as an unpleasant experience by diabetes patients, and may lead to patients developing restraints towards preforming BG measurements. Recent technological advancements have produced alternative ways to preform these measurements, allowing for a more comfortable experience for the patients. One of these advancements are the Continuous Glucose Monitor (CGM). The CGM is a small sensor installed under the patient's skin monitoring the subcutaneous glucose consecration of the interstitial fluid [22]. The CGM does not measure the BG directly but rather trough a proxy measurement, causing a delay between the actual BG concentration the CGM measurement [23]. The CGM sensor measures the subcutaneous glucose concentration at a regular time interval, every minute to every three minutes depending on the specific device used. In addition to the delay associated with these measurements so may they also be effected by electrical noise form the device itself.

2.2.3 Insulin Pump

In addition to the CGM, another technological milestone in the field of diabetes treatment is the introduction of the *Insulin Pump*. The insulin pump is a device that helps automate the insulin delivery process for the patient. It consist of a small tube connecting the insulin absorbing fatty tissues of the pancreas to an external pump that regulates the flow of insulin [22]. The pump allows the patient to specify the amount of insulin to be injected and takes care of the delivery process itself. This is, in most cases, a better alternative than the traditional method of delivering insulin through needle injections. Nowadays, most T1DM patients have the option to install a CGM and an insulin pump, and it is shown that such technologies improve the life quality of the patients [24].

2.3 Artificial Pancreas System

By combining the CGM and the insulin pump, and connecting them to a control algorithm, it is possible to construct a fully automated closed loop control system for diabetes treatment. The CGM measures the BG and feeds the data into the control algorithm, which in turn specifies how to adjust the flow of insulin to the Insulin pump based on these measurements [22]. System like these are called *Artificial pancreas systems*, and aim to artificially mimic the responsibilities of the pancreas in a healthy body. A simple illustration of the system can be found in figure 2.1. A closed loop system like this would ideally be able to calculate and deliver the optimal amount of insulin to keep the users BG levels in the hypoglycemic range range at all times, solely based on the CGM measurements, and regardless of the specific situation and lifestyle of the patient [9; 25].

New treatment approaches like artificial pancreas systems and other similar systems are in the forefront of modern diabetes research, and studies done on these topics have shown promising results, reporting both safety and effectiveness in improving glycemic control [9]. Extensions of the system has also been suggested, expanding it to a more general mobile health system that can give recommendations on a wider range of aspects related to the users health, like optimal food intake, physical exercise etc. based on health data collected by wearable devices like sports watches [9; 26].

The control algorithm functions as the main actor in an artificial pancreas system, deciding how much insulin to give the user at any given time, and therefore, how this algorithm is developed determines how safe and effective the system is. Over the years, several algorithm types have been used for this,

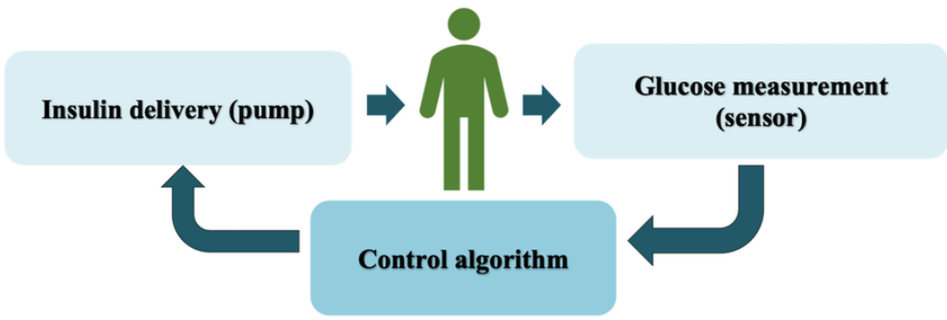

Figure 2.1: Illustration of an artificial pancreas system [27].

like model predictive controllers, proportional-integral-derivative controllers, and recently machine leaning based control methods like reinforcement learning have gained wide popularity in this field. One of the previously popular controllers used is the basal-bolus controller, a control algorithm based on the basal-bolus insulin regime that aims to recreate the effects by following this treatment regime.

/3

The Glycemic Index

As previously mentioned, the main way glucose is introduced to the body is through carbohydrate rich meals. However, not only the quantity of carbohydrates in a meal effects the following glycemic response, but also the quality of the carbohydrates consumed. The rate at which carbohydrates are digested and absorbed into the bloodstream depends on the type and complexity of the carbohydrates. Bigger and more complex carbohydrates take longer to be digested and absorbed than smaller, less complex carbohydrates. To capture this effect, the Glycemic Index (GI) was introduced in 1981 by David J. Jenkins et al. [28]. The GI works as an estimation of how quick the carbohydrates of a certain type of food are broken down under digestion and how fast they are absorbed into the bloodstream [29; 30], determining the rate at which carbohydrates effects the BG concentration [31].

Foods with high GI will be quickly broken down and absorbed into the bloodstream relative to low GI foods, resulting in an quick spike in BG concentration followed by a characteristic crash (BG concentration levels lower than fasting levels), before slowly stabilizing. In contrast low GI foods take longer to be broken down under digestion and are absorbed more slowly into the bloodstream than high GI foods, thereby resulting in a slower and more stretched out increase in BG levels as seen in figure 3.1. Now, other factors like protein, fiber and fat contain will also effect the foods GI.

The Glycemic Index is defined as the incremental area under the postprandial BG curve after eating 50g carbohydrates of a test food vs eating 50g carbohy-

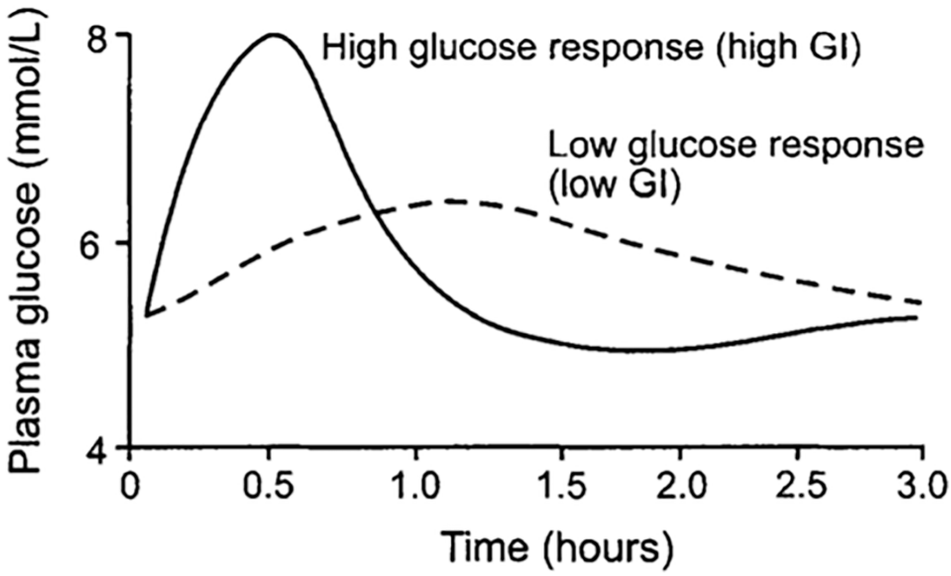

Figure 3.1: Typical postprandial BG curves of foods with high vs low GI [32].

drates of a control food (pure glucose or white bread). Both scenarios, control and test, needs to be carried out by the same subject as BG response is highly individual and may vary drastically form person to person. A 10-12 hour period of fasting is recommended before the scenarios to ensure the same prerequisites. When calculating the incremental area under the curve only BG values form the first two hours after consumption are considered, and only values above fasting BG [33]. The final GI is given by 3.1 and represented as an number between 0 and 100, where values less then 55 are considered low and values above 70 are considered high [34].

$$GI = \frac{AUC(BG_{test})}{AUC(BG_{Control})} \cdot 100 \tag{3.1}$$

To ensure a more general solution the test scenarios should repeated at least three times per subject and food, and the results should be average over a large population of subjects to get the final GI value [33]. Glycemic Index is not commonly listed among the nutritional contents on food labels like the amount of calories and such, but can be easily found online. Studies like [35] have been done reporting the GI of over 1500 different foods products.

If a food has a GI of 100 then it's equivalent to eating glucose, and if the food has a GI of 0 then the food will have no effect on the postprandial BG response. Now, when it comes to the effect a food has on the BG response, then the Glycemic Index is still only half the equation, as the quantity of carbohydrates

consumed still matter. Eating a small portion of a food with high GI will often result in less response on the postprandial BG than eating a large portion of a food with low GI. In other words, both the type of food and the portion size effects the BG response. To try to capture the full picture of the consumed foods effect on the BG response, the Glycemic Load (GL), an extension of the Glycemic Index concept was introduced, taking the amount of carbohydrates consumed into consideration. The Glycemic Load (GL) of a food is defined by equation 3.1, where *CHO* is the amount of carbohydrate (in grams) per serving [35].

$$GL = CHO \cdot \frac{GI}{100} \tag{3.2}$$

4

In-Silco Blood Glucose Simulation

Around the end of the century, the pursuit of developing In-Silco blood glucose simulators escalated in hopes of furthering our knowledge of the glucose-insulin system, and work as a safe alternative for experimental treatment trials. The availability of realistic In-silco BG simulators is quite useful when performing early trials for new technologies such as testing new glucose sensors, insulin infusion algorithms, and control algorithms for artificial pancreas systems [36], allowing trials that otherwise may have been structurally difficult to preform, inconvenient or potentially dangerous for the participants, to be preformed on an desired in-silco population. However, In-vivo clinical trials are still required for final validations [9].

Three main simulation models have gained international recognition over the years. The first among these was the Bergman's minimal model [37], a simplistic model comprised by a two separate compartmental-subsystems of linear differential equations. The first compartment describes the dynamics of plasma glucose uptake in response insulin concentrations, and the second describing the dynamics of pancreatic insulin secretion in response to the plasma glucose concentrations [9; 38]. The second of the main simulation models is the Hovorak model [5]. This model is comprised by five compartmental subsystems describing "subcutaneous insulin absorption, interstitial glucose kinetics, insulin actions, glucose kinetics and glucose absorption form the gas-

trointestinal tract" [9]. The third main simulation model, and only simulator to be approved by the The United States Food and Drug Administration (FDA) is the UVA/Padova model [7], described in detail in section 4.1.

4.1 UVA/Padova Simualtor

The UVA/Padova Type-1 diabetes simulator is a combined effort between researchers from the University of Virginia (US) and the university of Padova (Italy). It is the only BG simulator to date to be approved by the FDA for usage in pre-clinical trials, leading to the simulators wide popularity in the field of diabetes research. A virtual population of 100 children, 100 adolescent and 100 adult subjects is included in the simulator, and new virtual subjects can be produced by sampling a joint parameter distribution. The simulator also includes implementation of some well known CGM's and insulin pumps, and incorporates the delay and inherent noise associated with these, making for a more realistic simulation [22; 9].

The UVA/Padova's simulation model splits the glucose-insulin system into 10 compartmental subsystems describing; glucose kinetics, insulin kinetics, glucose rate of appearance, endogenous glucose production, glucose utilization, renal excretion, glucagon kinetics and secretion, subcutaneous insulin kinetics, subcutaneous glucose kinetics and subcutaneous glucagon kinetics [7]. The first 7 subsystems describe the internal part of the glucose-insulin system, while the last three describe the external parts, i.e. the subcutaneous glucose, insulin and glucagon kinetics effecting the CGM measurements and the insulin infusion [9].

The type-1 diabetes simulator was first introduced in 2008 and later improved upon in 2013. The 2008 version was based on an earlier simulator by the same group, called the *Meal Simulation Model of the Glucose-Insulin System*, a simulation model of the glucose-insulin system in healthy and type-2 diabetes subjects [36]. The *meal simulation model of the glucose-insulin system* follows the same simulation model as the UVA/Padova Type-1 diabetes simulator, the only exception being the replacement of the subcutaneous insulin kinetics subsystem, describing the dynamics of insulin rate of appearance form external sources, with a subsystem describing insulin secretion from the pancreatic beta-cells [39].

An open source version of the UVA/Padova simulator implemented in python, exists in the form of Xie's simglucose [40]. This version only includes a virtual population of 10 children, 10 adolescent and 10 adults subjects, but does include 3 different CGM's and two insulin pumps, alongside a pre-implemented PID and

basal-bolus controller. simglucose allows the user to specify the carbohydrate intake of the subject through a pre-planned set of meals, and the amount of basal and bolus insulin to injected by the insulin pump under the simulation. The duration of the simulation may also be specified. The initial BG concentration at the start of the scenario may be specified if desired but is by default sett to be randomized around the specific subjects fasting BG concentration. The CGM's included are all implemented with an inherent random noise to resemble real world scenarios, however by specifying the seed of this randomness, the user can redo the same simulation with the same noise. simglucose is compatible with Gymnasium [41] making it ideal for research utilizing reinforcement learning and similar approaches [22].

4.2 Extensions

In-silco blood glucose simulators have come a long way over the years, allowing for more realistic simulations than ever before. However, some crucial aspects of a patients everyday life are still not accounted for in state of the art simulators like the UVA/Padova simulator. The effect of a foods GI and the effect of physical activity through exercise are among the aspects unaccounted and therefor thought to be the next steps for improving BG simulations. Extensions have been made to add the effect of physical activity to both the Hovorak and the UVA/Padova model [18; 1; 42] gaining broad recognition in the field. Two of these will be described in detail in the following sections. However, to the knowledge of the author, no extensions have been made to add the effect foods glycemic index to any of the previously mentioned BG simulators. One notable simulation model that includes the effect of the glycemic index is the Type-1 Diabetes Direct Simulator (T1DDS) [43], a simple BG simulator designed to be used in virtual therapy of type-1 diabetes patients. Additionally Noguchi et al. (2016), defined the food inputs to their simulator and artificial pancreas system in terms of standard food and portion sizes [4].

4.2.1 Physical Activity Extensions

The physical activity extensions aim to model the effect exercise has on the human glucose-insulin system, and incorporate it to already existing simulation models, using the Heart Rate (HR) to describe the intensity of the exercise. Physical activity causes increased glucose absorption by the muscle cells and has been associated with prolonged increased insulin sensitivity and insulin-dependent glucose uptake [1]. The effect of physical activity can be modeled and added to the UVA/Padova model simply through changes to the glucose utilization subsystem. The original form of this subsystem is de-

scribed mathematical by equations 4.1 - 4.3. This subsystem is divided into two compartments, the insulin-dependent glucose utilization, U_{id}, and the insulin-independent glucose utilization, U_{ii} [36].

$$U(t) = U_{ii}(t) + U_{id}(t) \tag{4.1}$$
$$U_{ii}(t) = F_{cns} \tag{4.2}$$
$$U_{id}(t) = \frac{V_{m0} + V_{mx} \cdot X(t) \cdot G_t(t)}{K_{m0} + G_t(t)} \tag{4.3}$$

The parameter F_{cns} describes the glucose uptake by the brain and erythrocytes, while the parameter V_{m0} and K_{m0} are the Michaelis–Menten parameters of glucose utilization at zero insulin action. V_{mx} is the disposal rate of insulin sensitivity. X represents the amount of insulin in the interstitial fluid, and G_t represents the glucose mass in plasma and slowly equilibrating tissues[1].

Breton's Physical Activity Model

An extension to account for the effect of physical activity was first proposed for the Hovorak model by Marc D. Breton in 2008 [18]. A collaboration between Breton, Man & Cobelli later saw this physical activity model extended to the UVA/Padova model. The UVA/Padova version of Breton's PA model changes the insulin-dependent utilization of equation 4.3 to that of equation 4.4 [1].

$$U_{id}(t) = \frac{V_{m0}\,(1 + \beta \cdot Y(t)) + V_{mx}\,(1 + \alpha \cdot Z(t)) \cdot (X(t) + I_b) - V_{mx} \cdot I_b}{K_{m0}\,[1 - \gamma \cdot Z(t) \cdot W(t) \cdot (X(t) + I_b)] + G_t(t)} \cdot G_t(t) \tag{4.4}$$

Here, $X(t)$, $Y(t)$ and $Z(t)$ are given by equations 4.5-4.7, respectively. Note that a dot over a variable refers to its derivative. $W(t)$ is given by equation 4.9. β, α, γ are model parameters of Breton's PA extension and I_b is the basal plasma insulin concentration [1].

$$\dot{X}(t) = -p_{2U} \cdot X(t) + p_{2U}\,[I(t) - I_b] \qquad X(0) = 0 \tag{4.5}$$
$$\dot{Y}(t) = -\frac{1}{T_{HR}}\,[Y(t) - \Delta HR(t)] \qquad Y(0) = 0 \tag{4.6}$$
$$\dot{Z}(t) = -Z(t) \cdot \left[\frac{f(Y(t))}{T_{in}} + \frac{1}{T_{ex}}\right] + f(Y(t)) \qquad Z(0) = 0 \tag{4.7}$$

Breton model parmeters

Parameters:	Values:	Dimension
α	3×10^{-4}	1
β	0.01	bpm^{-1}
γ	1×10^{-7}	1
a	0.1	1
T_{HR}	5	min
T_{in}	1	min
T_{ex}	600	min
n	4	1

Table 4.1: Model parameters of the Breton physical activity model [42].

Where the parameter p_{2U} is the rate constant of insulin action on peripheral glucose utilization, and $I(t)$ is the currant plasma insulin concentration. T_{HR}, T_{in} and T_{ex} are further model parameters. $\Delta HR(t)$ stands for the change in heart rate and is defined as current heart rate, $HR(t)$ minus the base (resisting) heart rate, HR_b [1].

$$f(Y) = \frac{\left(\frac{Y}{a \cdot HR_b}\right)^n}{1 + \left(\frac{Y}{a \cdot HR_b}\right)^n} \tag{4.8}$$

$$W(t) = \begin{cases} \int_0^t \Delta HR(t) \cdot dt & \text{for } t < t_z \\ 0 & \text{otherwise} \end{cases} \tag{4.9}$$

Finally, the parameters a and n are also model parameters of Breton's PA model, and can be found in table 4.1.

Jaloli's Physical Activity Model

A new PA extension was released by Jaloli et. al in 2023 [42]. Jaloli's model features an PA model inspired by Breton's extension to the UVA/Paova model, with some slight adjustments based on newer development in the field. In contrast to Breton's model, Jaloli's model is evaluated by showing that the in-silco simulations are able to successfully recreate postprandial BG data seen in in-vivo subjects [42]. One key difference to the Breton model is that the Jaloli model assumes steady HR during exercise sessions, meaning that the intensity of the sessions are described by a step function with a magnitude equal to the average HR during the session. The Jaloli model also utilizes a patient specific β parameter, allowing for a better grasp the individual response

Jaloli model parmeters

Parameter:	**Value:**	**Unit:**
λ	1.2	1
β_{median}	0.0446	bpm^{-1}
ϵ	0.1	1
τ_h	10	min
τ_θ	180	min
κ	0.1151	min

Table 4.2: Model parameters of the Jaloli physical activity model [42].

to physical activity of subjects. Jaloli's PA model changes the insulin-dependent utilization of equation 4.3 to that of equation 4.10 [42]:

$$U_{id}(t) = \frac{V_{m0}\,(1+\beta\cdot h(t)) + V_{mx}\,(1+\lambda\cdot\theta(t))\cdot X(t)}{K_{m0}\,(1-\epsilon\cdot Z(t)\cdot w(t)) + G_t(t)}\;\cdot\; G_t(t), \tag{4.10}$$

where $X(t)$ is still given by equation 4.5 while $h(t)$ and $\theta(t)$ are given by equation 4.11 and 4.12, respectively, and β, λ and ϵ are the new model parameters.

$$\dot{h}(t) = -\frac{1}{\tau_h}\left[h(t) - \Delta HR(t)\right] \qquad h(0) = 0 \tag{4.11}$$

$$\dot{\theta}(t) = -\theta(t)\cdot\left[\varphi(t) + \frac{1}{\tau_{in}}\right] + \varphi(t) \qquad \theta(0) = 0 \tag{4.12}$$

Here, $\varphi(t)$ is given by equation 4.13 and $w(t)$ by equation 4.14. The parameters τ_h, τ_{in} and κ are additional model parameters of the Jaloli PA model, and can be found in table 4.2 alongside the median β reported in [42].

$$\varphi(t) = \frac{\Delta HR(t)}{1+\Delta HR(t)} \tag{4.13}$$

$$w(t) = \begin{cases} 0 & \text{prior to exercise} \\ \Delta HR(t) & \text{during exercise} \\ \Delta HR(t_{end})\,e^{-\kappa\,t} & \text{after exercise} \end{cases} \tag{4.14}$$

4.2.2 Digestion and Oral Glucose Absorption

One other important subsystem of the UVA/Padova simulation model, that will be needed when modeling the effect of foods glycemic index on the glucose-insulin system, is the Glucose rate of appearance subsystem. This subsystem models oral glucose absorption, describing the path of the carbohydrates through the human digestion system, from the time they are consumed until they are absorbed into the blood stream. The model breaks the digestion of carbohydrates down into three compartments, two for the stomach, describing both the solid and the triturated phase, and one for the intestine [44; 36; 7].

Immediately after ingestion, the carbohydrates, D, get introduced to the solid stomach compartment. From there, the carbohydrates are slowly ground down to monosaccharides while being introduced to the triturated stomach compartment. The rate at which they are ground down/introduced to the triturated compartment depends on patient specific rate of grinding parameter k_{gri}. The broken down carbohydrates (monosaccharides) are then passed on to the intestine, before being absorbed into the blood stream. The rate of gastric emptying, k_{empt}, determines how fast these broken down carbohydrates are passed to the intestine. Only once the carbohydrates have made there way to the intestine does the absorption process start. The rate at which the glucose is introduced to the plasma is determined by four factors, the amount of monosaccharides (glucose) in the intestine, Q_{gut}, the patient specific rate of intestinal absorption k_{abs}, the patient's body weight BW and a constant f representing the fraction of intestinal glucose that actually ends up in plasma, usually set to 0.9 meaning that 10% of the glucose in the intestine ends up somewhere else than the plasma. This process in mathematically described in equation 4.15-4.19 [44; 7; 1].

$$Q_{sto}(t) = Q_{sto1}(t) + Q_{sto2}(t) \qquad Q_{sto}(0) = 0 \quad (4.15)$$

$$\dot{Q}_{sto1}(t) = -k_{gri} \cdot Q_{sto1}(t) + D(t) \qquad Q_{sto1}(0) = 0 \quad (4.16)$$

$$\dot{Q}_{sto2}(t) = -k_{empt}(Q_{sto}(t)) \cdot Q_{sto2}(t) + k_{gri} \cdot Q_{sto1}(t) \qquad Q_{sto2}(0) = 0 \quad (4.17)$$

$$\dot{Q}_{gut}(t) = -k_{abs} \cdot Q_{gut}(t) + k_{empt}(Q_{sto}(t)) \cdot Q_{sto2}(t) \qquad Q_{gut}(0) = 0 \quad (4.18)$$

$$Ra(t) = \frac{f \cdot k_{abs} \cdot Q_{gut}(t)}{BW} \qquad Ra(0) = 0 \quad (4.19)$$

Here, D is the amount of carbohydrates ingested. Now, as described above, during the digestion process, these carbohydrates are broken down to monosaccharides and absorbed as glucose into the blood stream. However, to keep a common language with the UVA/Padova model when describing the parame-

ters of the subsystem, both carbohydrates and monosaccharides will be referred to as "glucose". Continuing the description, Q_{sto1} is the amount of glucose in the solid phase of the stomach, while Q_{sto2} is the amount of glucose in the triturated phase of the stomach, Q_{sto} is the total amount of glucose in the stomach, and Q_{gut} is the amount of glucose in the intestine. k_{gri} is the rate of grinding, k_{abs} is the intestinal absorption rate, and Ra is the glucose rate of appearance in plasma.

The rate of gastric emptying parameter k_{empt} is non-linearly dependent on Q_{sto}. If the amount of glucose in the stomach is equal to the currant carbohydrate intake then, the rate of gastric emptying is at it's maximum k_{max}. However, as the glucose (carbohydrates) gradually make there way from the stomach to the intestine,- will the rate of gastric emptying decrees until it hits its minimum at k_{min}. Before k_{empt} again rises up to k_{max} as the amount of glucose in the stomach goes towards zero, making Q_{sto} equal to D again, as long as no new carbohydrates are ingested. Mathematically k_{empt} is represented by equation 4.20, where b and c are patient specific parameter describing the rate at which k_{empt} decreases and increases [44]. A graphic representation of the gastric emptying dynamics is shown in figure 4.1.

$$
\begin{aligned}
&k_{empt}(Q_{sto}(t)) = \\
&\quad k_{min} + \frac{k_{max} - k_{min}}{2} \cdot \Big(tanh\Big(\frac{5}{2 \cdot D(t) \cdot (1-b)} \left[Q_{sto}(t) - b \cdot D(t)\right]\Big) \\
&\qquad\qquad - tanh\Big(\frac{5}{2 \cdot D(t) \cdot c} \left[Q_{sto}(t) - c \cdot D(t)\right]\Big) + 2 \Big)
\end{aligned} \tag{4.20}
$$

Finally for the purpose of ensuring that the models was uniquely identifiable it was assumed that $k_{gri} = k_{max}$ [44].

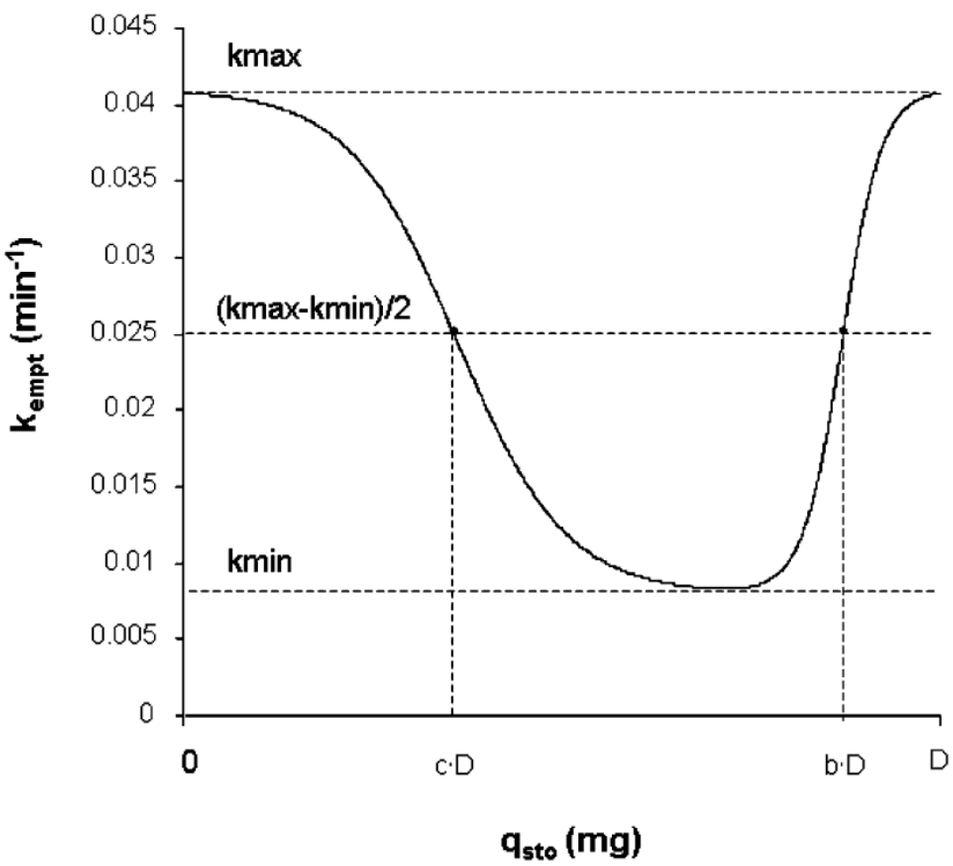

Figure 4.1: Plot of the gastric emptying rate k_{empt} as a function of Q_{sto} [44].

5

Artificial Neural Networks

Artificial Neural Networks are computational models that excel at learning intricate patterns in data [45]. This ability to learn patterns allows NNs to be used for a wide range of tasks like preforming predictions, classifications, data generations, decision support, etc. Making NNs an integral part in the development of modern Artificial Intelligence (AI) systems. There exists several types of NNs, each with their unique architecture and design, and with different aspects they excel at. However, in this section we will only look at the standard Feed Forward Neural Network (FFNN).

The FFNN is the predecessor of all NNs, and thereby often considered the simplest among them. Its design is inspired by the complex network of neurons in the human brain, and consists of layers of interconnecting nodes, as illustrated in figure 5.1. Each connection in the network is associated with a unique weight and each node in the network is associated with a unique bias. Together, these weights and biases determine the strength of the signal that passes through the nodes. Learning these weights and biases allows the system to learn intricate patterns that can be used to preform certain tasks [46].

Training a NN involves repeatedly sending data through the network to obtain an estimate of its error, called the loss, and updating the weights and biases in regards to this loss. The process this is done through is called *backpropagation*. It calculates the gradients of the loss based on the individual weights and biases, and updates them accordingly by using *gradient decent*, gradually moving towards the global minimum loss [46].

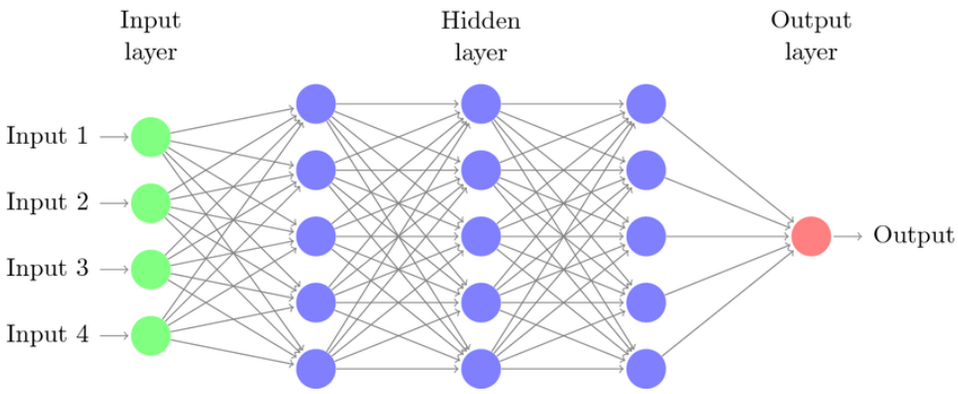

Figure 5.1: Diagram of a three layer Feed Forward Neural Network with five nodes per layer, four inputs, and one output [47].

The nodes are the building blocks of the network, and consist of a single perceptron each, which is why FFNN often are known as *Multi Layered Perceptrons*. These perceptrons preform a linear mapping of their respective input based on weights and biases associated with the nodes and the connections going into the nodes. In addition an activation function is commonly used to squeeze the mapping output into a desired range and add some non-linearity to it. By combining all of this, can we define the output of node k in layer l of a arbitrary FFNN by equation 5.1, where $y_k^{(l)}$ is the output of the node, $x_k^{(l)}$ is the inputs, ${}_k^{(l)}w$ and $b_k^{(l)}$ are the weights and biases and $N^{(l-1)}$ is the amount of nodes in the layer prior to l [46].

$$y_k^{(l)} = f\left(b_k^{(l)} + \sum_i^{N^{(l-1)}} w_{k,i}^{(l)}\, x_{k,i}^{(l)}\right) \tag{5.1}$$

By combining multiple perceptrons, all learning a linear mapping, the network can, as a whole, learn a non-linear mapping. Adding an activation function introduces more non-linearity to the network (as long as it itself is not linear) helping it learn these non-linear mappings quicker. The amount of layers and the number of nodes to use per is up to the designer. More layers and more nodes, lead to bigger and more complex networks. These bigger networks are capable of learning more complex patterns than smaller networks, but they also include more parameters that need to be learned, thereby requiring a longer training with more data to train on than a smaller network would need. In theory, a one layer network would be capable of learning any mapping arbitrary well, regardless of its complexity given enough data and enough training time. However, utilizing more layers will reduce the amount of data and training needed to achieve the same results [46].

Part II

Proposed Glycemic Index Extension

6

Methodology

To incorporate the effect of foods Glycemic Index into the UVA/Padova model, modifications were made to the *glucose rate of absorption subsystem*. Specifically, the rate of grinding and rate of intestinal absorption parameters were adjusted to better comply with literature. Literature states that GI affects the rate carbohydrates are broken down during digestion and the rate at which these broken down carbohydrates subsequently are absorbed into the bloodstream [29; 30] (see chapter 3 for further explanation). These physiological processes are already represented in the *glucose rate of absorption subsystem* through equations 4.16 - 4.19, where the rate of grinding k_{gri} and the rate of intestinal absorption k_{abs} control the speed of the processes. Thus, by adjusting k_{gri} and k_{abs} based on foods GI, it is possible to model the effects described in the literature into the simulator. To determine how to appropriately modify these parameters, assessments of the two boundary cases were conducted, looking at what would happen when GI equals 0 and 100.

The effect food has on the BG response is highly individual, and may vary drastically from patient to patient. Some patients may spend longer time digesting foods then others, some may be more affected by the carbohydrates they consume, and others may be less affected and depending on the severity of the disease, some patients may better respond to increased BG values. All these parameters and more will affect a patients BG response. It is therefor important to consider these individualities when modeling how to adjust the rate parameters for different GIs. A modeling scheme where the original values of k_{gri} and k_{abs}, simply are scaled based on the GI was therefore chosen.

These parameters are patient specific and are hence individual to each patient. Modeling foods with different GIs by simply scaling these parameters allows the patient specific response to be extended to foods with other GIs.

Xie's *simglucose* [40], the open source version of the UVA/Padova simulator, was used to implement and model the proposed GI extension. The code of the extension can be found in the A.1, along with a summery of the modifications done.

6.1 Boundary Assessment

For the upper boundary, we look at what happens when the GI reaches 100. The Glycemic Index is defined as the incremental area under the postprandial BG curve compared to a fixed control food and is given by equation 3.1. Thus, if a food has a GI equal 100, then that means that the glycemic response gained from consuming said food is identical to the response gained from consuming the control food. Commonly, either white bread or pure glucose is used as the control food, in our case we assume that pure glucose was used. Additionally, we assume that the parameters of the UVA/Padova model was modeled on data from glucose tolerance tests. Meaning that k_{gri} and k_{abs}, in their original form, were modeled on data from in-vivo patients consuming pure glucose which we already have determined to have a GI of 100, and therefore these parameters should stay unchanged in this case.

For the lower boundary, things get a bit more challenging. Here, we look at what happens when GI reaches 0. A Glycemic Index equal to zero means that the food consumed has no effect on the BG response. Therefor, when consuming zero GI foods, the rate of glucose appearance Ra should stay at zero. Ra, described by equation 4.19, is only equal to zero if either the amount of broken down CHO in the intestine Q_{gut} is zero or if the rate of intestinal absorption k_{abs} is zero. Now, foods that have a GI of zero usually do not contain any carbohydrates, or if so, only contain negligible amounts. These types of foods would not introduce any carbohydrates to the system, as no carbohydrates were consumed, and therefor Q_{gut} and Ra will stay at zero. However, consumption of a carbohydrate rich food with GI equal to zero should still result in no glucose appearing in the plasma. The only way to force Q_{gut} to stay at zero for carbohydrate rich meals is by scaling the rate of grinding, k_{gri}, to zero, thereby ensuring that the consumed carbohydrates are not broken down into absorbable monosaccharides. In conclusion, when the GI reaches zero, either one of the the rate parameters, k_{gri} or k_{abs}, controlling the flow of carbohydrates through the system, need to be scaled to zero.

6.2 Handling Meals with different Glycemic Indexes

A standard day is usually comprised of multiple meals which generally differ from another. The same type of food eaten at breakfast may not be present at dinner. So to accurately depict a day in the life of a patient, the proposed extension has to be able to handle scenarios with multiple meals of varying GI.

Let us consider an example scenario where two meals are consumed. The first meal, *Meal A*, consists of 40g CHOs with a GI of 30. The second meal, *Meal B*, consists of only 20g CHOs but with a GI of 75. *Meal A* is bigger and has a lower GI than *Meal B*. It will therefore take longer for *Meal A*'s carbohydrates to be digested and absorbed into the bloodstream than it will for *Meal B*'s carbohydrates. To model the different digestion and subsection absorption rates, the rate parameters k_{gri} and k_{abs} controlling the flow of carbohydrates through the system need to be scaled according to the meal's GI.

When the first meal is consumed, the rate parameters need to be scaled according to *Meal A*'s GI to comply for the rate its carbohydrates flow through the system. When the second meal is consumed, the rate parameters need to be scaled again to comply for the rate *Meal B*'s carbohydrate flow through the system if *Meal A* is fully digested and absorbed by the time *Meal B* is consumed. The rate parameters can, in this case, be safely rescaled according to *Meal B*'s GI. However, if some carbohydrates from *Meal A* is still in the system by the time *Meal B* is consumed, an issue occurs. Because once the carbohydrates are introduced to the system, there is no way of classifying which carbohydrates belong to which meal. This is an issue since the carbohydrates belonging to the different meals should be digested and absorbed at different rates.

Due to this issue, meals with different GIs need to be handled separately. The digestion and subsequent absorption of *Meal A* and *Meal B*'s carbohydrates, need to be calculated separately from each other to accurately depict the different rates these meals affect patients' BG.

To account for this, the *glucose rate of appearance subsystem* was expanded. The calculations of the subsystems were split into multiple channels, one channels for each GI considered. This allows foods with different GIs to be calculated independently of each other, accurately depicting the different rates this food would flow through the system. This does however require the previously continuous GI-space to be discretized based on the amount of chosen channels. The more channels chosen, the better the coverage of the GI-space becomes. However, more channels also makes the subsystem more computational ex-

pensive, as each channel adds three additional differential equations and a rate of appearance calculation. Equation 6.1 to 6.4 summarize the calculations done per channel. These are identical to equation 4.16 to 4.19 of the original subsystem, the only difference being that the equations now are conditioned on a specific GI to keep each channel distinct.

$$\dot{Q}_{sto1}(t, GI) = -k_{gri}(GI) \cdot Q_{sto1}(t, GI) + D(t, GI) \qquad Q_{sto1}(0, GI) = 0 \tag{6.1}$$

$$\dot{Q}_{sto2}(t, GI) = -k_{empt}(Q_{sto}(t)) \cdot Q_{sto2}(t, GI) + k_{gri}(GI) \cdot Q_{sto1}(t, GI) \qquad Q_{sto2}(0, GI) = 0 \tag{6.2}$$

$$\dot{Q}_{gut}(t, GI) = -k_{abs}(GI) \cdot Q_{gut}(t, GI) + k_{empt}(Q_{sto}(t)) \cdot Q_{sto2}(t, GI) \qquad Q_{gut}(0, GI) = 0 \tag{6.3}$$

$$Ra(t, GI) = \frac{f \cdot k_{abs}(GI) \cdot Q_{gut}(t, GI)}{BW} \qquad Ra(0, GI) = 0 \tag{6.4}$$

Each channel of the expanded *glucose rate of appearance subsystem*, only models the digestive and subsequent absorption processes of foods with a GI specific to that channel. To summarize the whole subsystem and to model the full oral glucose absorption process, all channels need to be summed together, thereby making equation 6.5 to 6.9, the final output of the system. Here $\mathbb{C}$ is chosen to depict the discrete GI-space. It is important to note that the gastric emptying rate, k_{empt} used within the channels should not be calculated individually per channel, but rather across all channels as it is non-linearly dependent on the **total** amount of carbohydrates in the stomach.

$$Q_{sto}(t) = Q_{sto1}(t) + Q_{sto2}(t) = \sum_{GI \in \mathbb{C}} Q_{sto1}(t, GI) + Q_{sto2}(t, GI) \qquad Q_{sto}(0) = 0 \tag{6.5}$$

$$\dot{Q}_{sto1}(t) = \sum_{GI \in \mathbb{C}} \dot{Q}_{sto1}(t, GI) \qquad Q_{sto1}(0) = 0 \tag{6.6}$$

$$\dot{Q}_{sto2}(t) = \sum_{GI \in \mathbb{C}} \dot{Q}_{sto2}(t, GI) \qquad Q_{sto2}(0) = 0 \tag{6.7}$$

$$\dot{Q}_{gut}(t) = \sum_{GI \in \mathbb{C}} \dot{Q}_{gut}(t, GI) \qquad Q_{gut}(0) = 0 \tag{6.8}$$

$$Ra(t) = \sum_{GI \in \mathbb{C}} Ra(t, GI) \qquad Ra(0) = 0 \tag{6.9}$$

It was chosen to use a total of 101 channels for the extended *glucose rate of appearance subsystem*. One channel for each whole number the GI can take, thereby defining the interval $\mathbb{C}$ as follows:

$$\mathbb{C} = [0, 1, 2, 3, \ldots, 100]. \tag{6.10}$$

Though the GI does not technically need to be whole number, it is usually represented as such in listings.
The total amount of differential equations in the *glucose rate of appearance subsystem* will then increase to 102×3, as the three equations summarizing the flow across all channels also have to be represented as differential equations in the system.

6.3 The Lower Boundary Issue

We previously stated that in cases where zero-GI foods are consumed, either k_{gri} or k_{abs} should be scaled to zero to ensure that the no glucose appears in the plasma. The issue is that scaling any of these rate parameters to zero will result in the carbohydrates associated with the zero GI food getting stuck somewhere in the system. If k_{gri} is scaled to zero, the carbohydrates will get stuck in the solid stomach compartment, unable to move further and therefor always effecting Q_{sto1}. Conversely, if k_{abs} is scaled to zero, the carbohydrates will get stuck at the intestinal compartment, unable to move and always effecting Q_{gut}.

This issue arises due to the way the simulator is modeled. The UVA/Padova model only considers the path digestible carbohydrates take up until they are absorbed by the intestine. Bowel movements or gastric emptying of non-digestible carbohydrates are not included in the model.

Scaling either of the rate parameters to zero is therefor problematic. However, we will see that carbohydrates stuck in the intestinal compartment will not affect future simulations, and will therefor be less problematic than carbohydrates stuck in the solid stomach compartment as these will affect future simulations.

This is due to how meals with different GIs are handled in the proposed extension. Since foods with different GIs are modeled separately in different channels, the carbohydrates will get stuck due to consumption of zero GI meals, specifically, they are stuck the channel responsible for these types of meals, in other words, the zero GI channel. The stuck carbohydrates will cause the amount of carbohydrates in its channel compartment to be permanently increased. Meaning that if carbohydrates get stuck in the channels solid stomach compartment due to scaling k_{gri} to zero, $Q_{sto1}(t, GI = 0)$ will be increased permanently. And similarly, if carbohydrates get stuck in the channel's intestinal compartment due to scaling k_{abs} to zero, $Q_{gut}(t, GI = 0)$ will be permanently increased.

A permanent increase to either $Q_{sto1}(t, GI = 0)$ or $Q_{gut}(t, GI = 0)$ will not affect the calculations of the zero GI channel. Within each channel, $Q_{sto1}(t, GI)$ only appears together with $k_{gri}(GI)$, and $Q_{gut}(t, GI)$ only appears together with $k_{abs}(GI)$. Since $k_{gri}(GI = 0)$ is set to zero in cases where $Q_{sto1}(t, GI = 0)$ is increased, and $k_{abs}(GI = 0)$ is set to zero in cases $Q_{gut}(t, GI = 0)$ is increased, the channel specific rate parameters will make the increased carbohydrate amounts of the channel's compartments insignificant.

Each channel of the extended *glucose rate of appearance subsystem* models the flow of carbohydrates separately from each other, so an incorrect value in one channel may not necessarily cause issues for the other channels. The issue of carbohydrates getting stuck is specific to zero GI meals, as these are the only cases were the rate parameters are scaled to zero. This means that only the zero GI channel will experience permanent increases to its compartment's carbohydrate content. Other, non-zero GI channels will not experience this. However, increasing the amount of carbohydrates in a specific channel's compartment will also increase the total amount of carbohydrates in that compartment across all channels. So modeling lower boundary cases by scaling k_{gri} to zero will not only cause $Q_{sto1}(t, GI = 0)$ to be permanently increased by the carbohydrates of the zero GI meals, but also $Q_{sto1}(t)$. Similarly, modeling lower boundary cases by scaling k_{abs} to zero will also lead to a permanent increase of $Q_{gut}(t)$

caused by the carbohydrates of zero GI meals.

The only part of the digestive and subsequent absorption process that is not modeled individually per channel is the gastric emptying rate, k_{empt}. This parameter is dependent on the total amount of carbohydrates in the stomach, $Q_{sto}(t) = Q_{sto1}(t) + Q_{sto2}(t)$. In other words, it is dependent on the total amount of carbohydrates in both the solid and triturated stomach compartments across all channels. Carbohydrates stuck in the zero GI channels solid stomach compartment, will permanently increase the total amount of carbohydrates in the stomach and will therefor introduce errors to the gastric emptying rate calculations as the amount of carbohydrates currently in the stomach, $Q_{sto}(t)$, no longer can be equal to the amount of carbohydrates currently consumed $D(t)$. Since all channels depend on the same gastric emptying rate, this error will affect the flow of carbohydrates in all channels for all future non-zero GI meals. Therefor, k_{gri} can not be scaled to zero to model lower boundary cases.

Carbohydrates stuck in the intestine compartment will not affect the gastric emptying rate, as they do not count towards the total amount carbohydrates in the stomach. Additionally, no part of the simulation model actually depends on $Q_{gut}(t)$, the total amount of carbohydrates in the intestinal compartment across all channels as the rate of glucose appearance, Ra, is calculated individually within each channel, only using the individual channels $Q_{gut}(t, GI)$ and $k_{abs}(GI)$ parameters. Therefore, k_{abs} may safely be scaled to zero to model lower boundary cases, without affecting the flow of carbohydrates for future meals since the only parameter permanently affected by the carbohydrates stuck in the intestinal compartment is a dead parameter that is not used for anything in the model.

It is also worth noting that these lower boundary cases can not simply be ignored. As cases where zero GI foods are consumed, are not identical to cases where no foods are consumed, even though both cause the same Ra. In cases where zero GI foods are consumed, carbohydrates enter the stomach, thereby effecting the gastric emptying rate, while cases where no foods are consumed will not effect the gastric emptying rate.

6.4 Modeling Technique and Evaluation Metric

We have now looked at how the rate parameters, k_{gri} and k_{abs}, should be scaled at the boundary cases of the GI-interval. We have defined that both k_{gri} and k_{abs} should keep their original value to model the upper boundary cases where the consumed meals GI equals 100. We have also seen that k_{abs} needs

to be scaled to zero, and not k_{gri}, to model the lower boundary cases where the consumed meal's GI equals 0. In this section, we will define the method used for modeling how the rate parameters should be scaled in cases between the two boundaries.

Before starting, it is important to define the value k_{gri} takes at the lower boundary. We have previously defined that k_{gri} should not be scaled to zero in these cases, as that would cause dependency errors in the system. However, it should also not stay at its original value, as the digestion of zero GI foods should take longer than the digestion of pure glucose. Because of this, the assumption made to k_{gri} in the UVA/Padova model was expanded upon (see section 4.2.2), changing it from $k_{gri} = k_{max}$, to $k_{gri} \in [k_{min}, k_{max}]$ and thereby choosing the patient specific minimum gastric emptying rate, k_{min}, as the lower boundary value of k_{gri}.

The literature states that food with higher GIs, should be digested faster and absorbed quicker than foods with lower GIs. This means that the functions $k_{gri}(GI)$ and $k_{abs}(GI)$ describing the new value of the rate parameters should be strictly increasing on the interval $GI \in [0, 100]$. The ranges of the new parameter values will thus be defined as:

$$k_{gri}(GI) \in [k_{min}, k_{max}] \qquad k_{abs}(GI) \in [0, k_{abs}]. \tag{6.11}$$

A simple scaling technique was then used to model the rate parameter functions in their respective ranges. The functions were chosen to fulfill the conditions mentioned above as well as the following boundary conditions:

$$k_{gri}(GI = 0) = k_{min} \qquad k_{gri}(GI = 100) = k_{max} \tag{6.12}$$

$$k_{abs}(GI = 0) = 0 \qquad k_{abs}(GI = 100) = k_{abs}. \tag{6.13}$$

The rate parameter functions are written as follows:

$$k_{gri}(GI) = \left(\frac{GI}{100}\right)^{\lambda_{gri}} \cdot (k_{max} - k_{min}) + k_{min}, \qquad \lambda_{gri} > 0 \tag{6.14}$$

$$k_{abs}(GI) = \left(\frac{GI}{100}\right)^{\lambda_{abs}} \cdot k_{abs}, \qquad \lambda_{abs} > 0. \tag{6.15}$$

λ_{gri} and λ_{abs} are positive scalars defining the shape of the functions. These are the parameters used to fit the extended simulation model to GI data and will therefor need to be optimized.

The glycemic index is calculated from the postprandial BG curve, using equation 3.1. It compares how the BG response gained from consuming $50g$ of a specific

food relates to the response gained from consuming the same amount of pure glucose. Thus, for the simulator to accurately model the effect a food's GI has on the glucose-insulin system, so should the GI calculated from the simulated BG response fit the GI of the simulated meal. If the simulated meal has a GI of 35, the GI calculated for the simulated BG response should also be 35. In other words, the closer the recalculated GI is to the GI of the meal originally simulated, the better is the fit of the simulator. Since we wish to make the model accurately depict foods with all the different GIs represented in $\mathbb{C}$, we must find the pair of λ_{gri} and λ_{abs} that produces the best cumulative fit for all the different GI.

The method used to evaluate the fit of the simulator for a single set of λ_{gri} and λ_{abs}s involved simulating single meal simulations for each of the unique GI in $\mathbb{C}$, and then recalculating the index based on the simulated BG data. The simulated meals were consumed 12 hours after simulation start, and included 50g of carbohydrates. This was done to ensure a common ground to compare the meals with an steady initial fasting BG level, thereby recreating the conditions for GI calculations described in chapter 3. The GI of the meals was recalculated using equation 3.1 and the simulated postprandial BG curves. Only values bigger than the fasting BG and in the first two hours after consumption were considered when calculating the area under the curves. Meals where the GI equaled 100 were used as a control and the different unique GI meals were used as test. The same set of λ_{gri} and λ_{abs} was used under each simulation. A mean squared error loss was used to describe cumulative error of the fit. The specific loss function used is described in equation 6.16 where GI is the meals actual glycemic index and $\hat{GI}$ is the recalculated glycemic index.

$$MSE = \sum_{GI \in \mathbb{C}} \left[GI - \hat{GI} \right]^2 \tag{6.16}$$

A simple grid search technique was used to find the optimal set of λ_{gri} and λ_{abs}. Both parameters were initially set to 1.0 and then slowly increased one by one until the optimal value was found.

6.4.1 Modeling Subjects

The Glycemic Index is not a measurement meant to be used specifically for diabetes patients, but rather for the whole human population. The calculation technique described by the United Nations Food and Agriculture Organization [33] is not suited to be used for diabetic patients as it only considers the BG response for the first two hours after consumption. Patients with diabetes are not able to produce sufficient amounts of insulin to control their BG concen-

trations and will therefor experience an increased and prolonged BG response compared to non-diabetic patients. A time frame of two hours will only cover a small fraction of this prolonged response, and will therefor be a bad depiction of the overall effect food has on the glucose-insulin system.

Because of the reasons mentioned above, it was decided to not use the in-silco T1DM patients included in *simglucose* to perform the modeling, but rather in-silco non-diabetic patients. These in-silco non-diabetic patients would first need to be added to the simulator for them to be used in the modeling of the extended *glucose rate of appearance subsystem*. Additionally, to adjust for the different physiology of these healthy non-diabetic subjects, so the *subcutaneous insulin kinetics subsystem*, describing insulin rate of appearance dynamics from external sources, was replaced with the subsystem describing insulin secretion from the pancreatic beta-cells included in the *Meal Simulation Model of the Glucose-Insulin System* [36; 39].

The only model parameters of a non-diabetic patient available to the author at the time of writing were the ones given for the *Normal* patient in Table 1 of Man et al. (2007) [36]. These are the average model parameters of the 204 healthy subjects included in the *Meal Simulation Model of the Glucose-Insulin System* [36]. Not all model parameters required by *simglucose* are given in Man et al. (2007) [36], so the parameters missing needed to be calculated. This was done by using the basel state equations listed in [7; 1; 36; 39].

Simulated data from the added non-diabetic patient was then used to model the extended *glucose rate of appearance subsystem*, finding the λ_{gri} and λ_{abs} that optimizes the fit the proposed extensions simulated data. The *subcutaneous insulin kinetics subsystem* was only replaced during the modeling phase. It was replaced back after the modeling was finished to allow the simulation of T1DM patients.

7

Results

In this chapter, we will present the results for the proposed GI extension, building on the methodology outlined in chapter 6. We will first present the result of the GI molding before looking at simulations of this modeled extension. The modeling was performed using the technique and evaluation criteria described in section 6.4 on simulated data from the added non-diabetic subject described in section 6.4.1. The results are briefly explained as they are presented and will be discussed in more detail in chapter 8.

7.1 Modeling Results

The values of λ_{gri} and λ_{abs} found to optimize the cumulative fit of the simulated meals GI and their following BG responses are as follows:

$$\lambda_{gri} = 4.0, \qquad \lambda_{abs} = 1.2. \tag{7.1}$$

This causes the rate parameter functions describing the different rates carbohydrates of different GIs are digested and absorbed, to be as follows:

$$k_{gri}(GI) = \left(\frac{GI}{100}\right)^{4.0} \cdot (k_{max} - k_{min}) + k_{min} \tag{7.2}$$

$$k_{abs}(GI) = \left(\frac{GI}{100}\right)^{1.2} \cdot k_{abs}. \tag{7.3}$$

This will result in the rate of absorption increasing almost linearly as the the food's GI increases, while the rate of grinding will increase slower in the lower

part of the GI spectrum and faster in the higher parts of the spectrum. Meaning that low and medium GI foods will have a rate of grinding close to k_{min}, while high GI foods will have a rate of grinding close to k_{max}.

Figure 7.1 summarizes the total fit of the modeling results for all GI values in the interval $\mathbb{C}$ by plotting the GI of the simulated meals against their recalculated value based on the simulated BG response. The diagonal blue line shows the optimal result where each recalculated GI value equals the GI of the simulated meal. The orange line shows our modeling results. The original GIs of the simulated meals are shown along the x-axis, and the recalculated values, $\hat{GI}$, are shown along the y-axis. The mean squared error of this fit was 1.380, meaning that the GI depicted by the simulated BG response is on average only $\sqrt{1.380}$ values different than the one actually simulated. We can see that our solution slightly diverges from the optimal one in three main regions, the first around $GI = 20$, the second around $GI = 55$ and the third around $GI = 85$. In the first and the last region, the GIs depicted in the BG response will be slightly higher than the ones of the consumed meal, and in the middle region the depicted GI will be slightly lower than those of the consumed meals. The simulated BG responses accurately depict the GI in the boundary cases as well as in the two spots our found solution crosses the diagonal. The values of k_{gri} and k_{abs} at the boundary cases are coded into the rate parameter functions and are therefor accurately fitted.

It is important to remember that the results illustrated in figure 7.1 only show the fit of cases used in the actual modeling process, meaning that all meals were simulated on the non-diabetic patient and had a carbohydrate content of 50 grams. Due to the issues discussed in section 6.4.1 regarding GI calculations from BG responses of patients with diabetes, it is not possible to evaluate the fit for data simulated from T1DM patients.

7.2 Simulation Results

Figure 7.2 and 7.3 showcase postprandial BG simulations of the modeled GI extension for both the non-diabetic patient and a arbitrarily chosen T1DM patient. The illustrated postprandial BG curves are simulated from single meal simulations with varying GIs where each meal contained 50g carbohydrates. The color of the curves represent the GI value of the simulated meal. The blue curves show the postprandial BG from zero GI meals and are in both cases simulated as a straight horizontal line along the fasting BG value of the respective patient. The orange curves show the postprandial BG of meals with a GI equal to 25. The green curves show the response from meals with a GI equal to 50. The red curves for meals with a GI equal to 75, and the purple curves

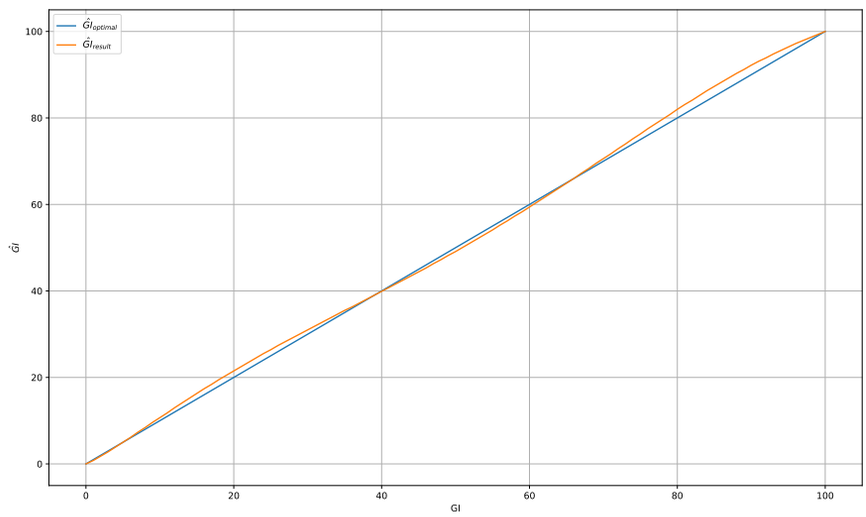

Figure 7.1: Modeling results of the GI extension. The GI of the simulated meals modeled are plotted against their recalculated values $\hat{GI}$. The diagonal blue line depict the optimal result where each recalculated value equals the GI of the simulated meal, And the orange line depicted our modeling results.

for meals with a GI equal to 100. For the T1DM simulation scenarios, a patient specific basal dose included in the Basal Bolus controller of Xie's *simglucos* [40] was administered to the patient to ensure steady fasting BG levels. No bolus doses were administered in the simulation scenarios.

It is evident from the figures that the GI extension is able to capture the described effect foods' GI has on the BG response in the literature. The postprandial BG simulations of high GI meals depicts a quick spike of large magnitude followed a drastic decrease in the BG concentrations, while the simulations of low GI meals depicts a slower, steadier and longer lasting increase of the patient's BG concentration with less amplitude than that of high GI meals. Both these observations comply with what is described in the literature.

The simulated postprandial BG curves of the non-diabetic patient also depict the characteristic crash seen in the BG concentration after consuming high GI foods, resulting in the BG concentration dropping lower than the fasting levels. This crash is caused by glucose homeostasis, the body's natural response towards changing BG levels. The body responds to the rapid increase in BG concentration by increasing the amount of insulin secreted by the pancreatic β-cells. High GI foods are quickly digested and absorbed, causing the body to secrete more insulin then needed to stabilize the BG concentration, which

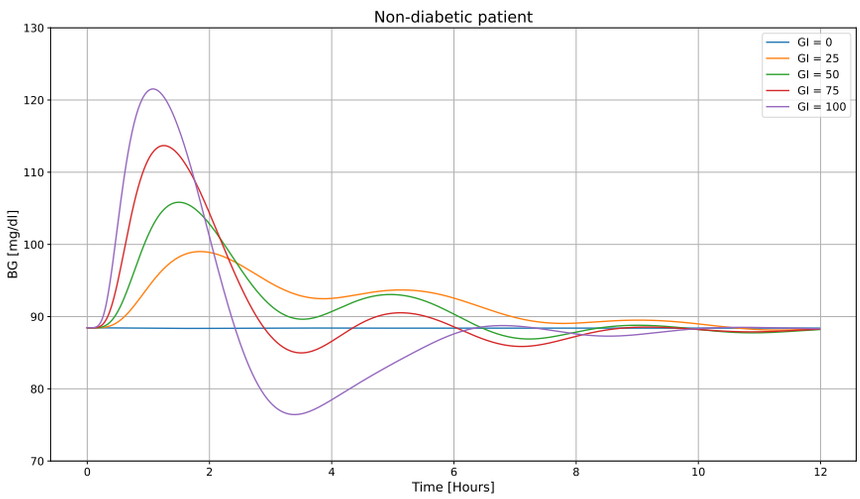

Figure 7.2: Postprandial BG simulations of meals containing 50g carbohydrates with GI equal to; 0, 25, 50, 75 and 100, for the non-diabetic patient.

in turn causes the characteristic crash. The body will then respond to these decreasing BG concentrations by increasing the amount of glucagon secreted by the pancreatic α-cells. These opposing insulin and glucagon actions are what is causing the stabilizing effect seen in the simulated BG responses of the non-diabetic patient. Patients with T1DM are not able to produce enough insulin to successfully respond to these increasing BG concentrations. We will therefor only see these effects in the postprandial BG curves of the non-diabetic patient, and not the T1DM patient.

The simulated BG responses of the T1DM patient, depicted in figure 7.2, are longer and of higher magnitude than those of the non-diabetic subject shown in figure 7.2. This is also as expected as the lack of insulin production will cause T1DM patients to be more affected by the consumed carbohydrates and makes them unable to lower these increased BG concentrations in a normal time frame.

The depicted increase to the BG concentration caused by the consumption of non-zero GI meals is on average three times higher for the T1DM patient than for the non-diabetic patient. It also takes the T1DM patient considerably longer to get the BG concentrations back to their fasting levels than the non-diabetic patient. For the non-diabetic patient, the BG concentrations are all stabilized within 12 hours after consuming the meals. However, the BG concentrations return to the fasting levels for the first time as early as 2.5 and 3.0 hours for the high GI meals ($GI = 100$ & $GI = 75$). For the T1DM patient on the other

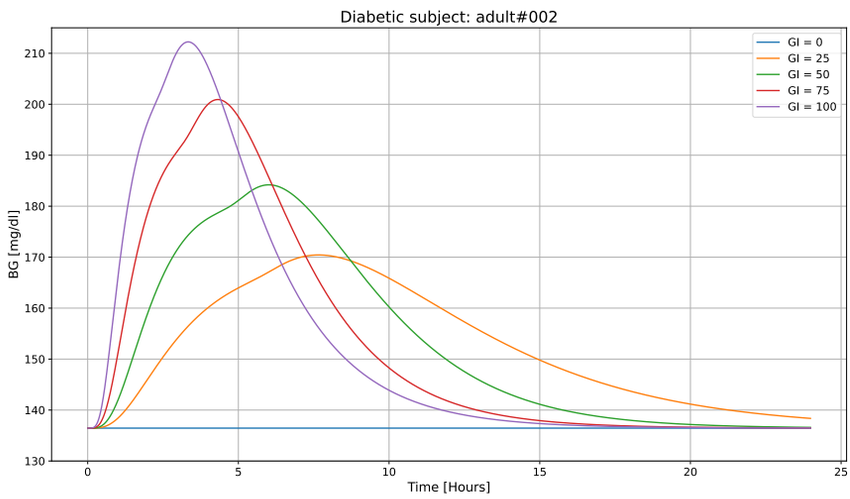

Figure 7.3: Postprandial BG simulations of meals containing 50g carbohydrates with GI equal to; 0, 25, 50, 75 and 100, for the T1DM patient: adult#002.

hand, it takes 20 to 24 hours for the BG concentration to get back to fasting levels for the majority of the meals and more than 24 hours for the meal with GI equal to 25. These simulated values will vary from patient to patient as they depend on the patient specific parameters.

The dip seen in the increase of all postprandial BG curves in 7.3 is caused by the gastric emptying process. As the stomach fills up with carbohydrates, the gastric emptying rate decreases causing a dip in the rate glucose appears in the plasma as the amount of carbohydrates in the stomach gradually decreases. Thus, the gastric emptying rate increases again, causing more carbohydrates to flow into the intestines to be absorbed.

8

Discussion

In this section we will discuss the methodology and results of the proposed GI extension presented in this thesis.

8.1 Glycemic Index's Effect on the Glucose-Insulin System

Glycemic Index is an end to end measurement that quantifies the effect different types of food have on the BG response. Only postprandial BG values are considered when calculating a food's GI. Even though these values give an indication to the rates foods are digested and subsequently absorbed, they do not specifically measure this. The GI therefor only works as an estimate of these rates but does not depict the full effect food has on the specific processes of the glucose-insulin system. The UVA/Padova model simulates a patient's BG by modeling these processes. The simulator splits the glucose-insulin system into 10 compartmental subsystem and models the effect external sources like insulin and meals carbohydrate content have on the system. So to add GI to the simulator, we had to model how it affected the different subsystems. In the methodology of section 6, we propose that only the *glucose rate of appearance subsystem* needs to be modified to add this effect. This subsystem is responsible for the digestion and absorption of carbohydrates and by changing the rates of these processes, we may depict the anticipated BG response of different GI

foods. How the GI affected the digestion and absorption of carbohydrates was the main focus in our extension. Any possible effect it may have on other parts of the system was only briefly considered. Further research should therefor be done on the topic to investigate alternative effects foods' GI may have on the system.

8.2 Modeling of the Lower Boundary

In the assessment of the lower boundary in section 6.1, we state that no glucose should enter the bloodstream due to the consumption of zero GI foods and that therefor either the rate of grinding, k_{gri}, or the rate of adsorption, k_{abs}, should be scaled to zero to model these cases, thereby ensuring that the glucose rate of appearance, Ra, stays at zero. However, due to the issue explained in section 6.3, we were forced to model these cases by scaling k_{abs} to zero and not k_{gri}. This was done out of necessity as scaling k_{gri} to zero would have caused permanent errors to the gastric emptying rate, which would affect all other meals simulated in the same scenario. It was therefore chosen to set k_{gri} equal to the minimum gastric emptying rate k_{min}, for the lower boundary cases, expanding on the assumption made the original model.

However, if we consider what type of food actually has a GI equal to zero, it would theoretically make more sense for the rate of grinding to be zero in these cases than for the rate of absorption. Foods commonly labeled as zero GI foods usually contain no carbohydrates, like meats and fats, and if they do so, they only contain negligible amounts. These foods would not introduce any carbohydrates to the system, and therefore no glucose would end up in the plasma due to them. Though as previously mentioned, consuming a carbohydrate rich meal with GI equal to zero should also result in now glucose appearing in the plasma. But what would such a food be? And does such food even exist? This is a bit unclear, as no foods containing a significant amount of carbohydrates are listed to have a GI of zero in the international GI tables [35]. However, it is not unreasonable to think that foods containing mainly carbohydrates that are not digestible for the human body, like cellulose, would qualify as zero GI foods. The human body would not be able to break down these carbohydrates to absorbable monosaccharides, and therefor no glucose would appear in the plasma due to them. Following this logic, it would theoretically make more sense that k_{gri} would be zero in these cases as it represent the rate at which these carbohydrates are broken down, and since the body can not break these carbohydrates down, the rate of grinding wold theoretically be zero. These are all still speculations, and more research needs to be done on the topic to figure out what these zero GI foods represent and if it is needed to cover them in the model. But if this is the case, would we

recommend adding gastric emptying of non-digestible carbohydrates and bowl movements into the model to make the final model more theoretically accurate and thereby allowing k_{gri} to be zero.

8.3 The Glucose Tolerance Test Assumption

When molding the proposed extension, we assumed that the parameters of the UVA/Padova simulator were modeled on glucose tolerance test data and that k_{gri} and k_{abs} should therefore keep their original value at the upper boundary. The glucose tolerance test is a common experiment where a patient consumes a specific amount of glucose while their BG concentrations are monitored. The test is used to check how the body handles glucose and is often used to diagnose diabetes in the early stages [48]. Due to the simplicity of this test and amount of available data from them, data from them are often used in the modeling of in-silco treatment strategies. Another popular data to use in the development of in-silco treatment strategies is mixed meal data. This data is similar to the glucose tolerance test data, but depict how a mixed meal affects the patients BG concentrations instead of pure glucose, thereby giving a better depiction of patients everyday life. The data used to model the UVA/Padova simulator was not available to the author at the time of writing. And to the knowledge of the author, it is never stated in the publicly available literature what was used. It was therefor assumed that glucose tolerance test data was used, as it aligned better with our intended goal. However, this assumption is not correct for the non-diabetic patient added from Man et al. (2007) [36], as this one is modeled on mixed meal data. The original value of k_{gri} and k_{abs} will therefore depict the mixed meals GI and not the GI of pure glucose ($GI = 100$). So to accurately model this patient, we should have used the mixed meals GI as the upper reference point instead of $GI = 100$. However, as the GI of the mixed meal is not known so was this not possible.

Now, since the non-diabetic patient is used to model the scaling of the rate parameter function for all of our patients, the significance of this incorrect assumption will be of importance. Due to the high glucose content of the mixed meals used, 1 ± 0.02 g per kg body weight [36], the GI of the mixed meal will be high, causing the incorrect assumption to have less significance.

Man et al. (2006) [44] conducted tests on oral glucose absorption models, looking at how these models fitted mixed meal and glucose tolerance test data. One of the models presented in the paper was the *glucose rate of appearance subsystem* used in the UVA/Padova simulator. This was also the model that best fitted both sets of data. Their results depict that the parameters modeled on mixed meal data slightly varies from those modeled on glucose tolerance test

data. k_{min} and k_{abs} were smaller for the mixed meal model than for the glucose tolerance test model. However, k_{max} which k_{gri} is assumed to be equal to, was found to not be significantly different in the two models. These results support our methodology as mixed meal have lower GI then pure glucose and therefor would have a lower absorption rate. Additionally, due to the inclusion of other nutrients such proteins and fats in the mixed meal, this would slow down the gastric emptying rate [44]. When applying these results to our situation, we see the incorrect assumption mainly affects the rate of absorption, as it theoretically should have been slightly higher than what is depicted in our results.

Even though the proposed extension might not be 100% correct, it depicts the desired effect the GI has on the BG response. This can be admired, and we hope our model can work as a proof of concept and a baseline for future GI extensions.

8.4 The Effects of Other Nutrients on the System

As demonstrated by last section, there is more than just the carbohydrates that affect a meal's BG response. Other nutrients, such as proteins and fats, will also affect the digestion of carbohydrates. Proteins and fats do not directly cause glucose to appear in the plasma, but both slow down the rate of appearance of glucose from other sources, such as carbohydrates. Both, protein and fats are digested in the stomach and therefore affect the gastric emptying rate as depicted in Man et al. (2006) [44]. Though the GI originally was presented as a measurement depicting how different types of carbohydrates affect the BG response, it is commonly calculated per food/meal. And as a food or a meal usually includes more than just carbohydrates, its GI will also include the effects of other nutrients present in the food or meal. It is therefore not necessarily needed to extend the simulator further to include the effect of proteins and fats as these are already modeled into the meals GI.

8.5 Optimization Technique

A grid search was used to perform the modeling of the extension. This technique is in no way the most effective optimization technique as it is time consuming and relies on trial and error. Though the results of the modeling depict a good fit, this may be more due to the luck of searching in the right area than due the performance of technique. A more sophisticated approach to the optimization would therefor be recommended, and would most likely result in

a better fit. However, as we are not able to differentiate through the simulator, standard machine learning optimizations techniques cannot be used for the modeling. One could do a similar approach to what was done to for the food recommendation systems by training a network to map pairs of λ_{gri} and λ_{abs}'s to the MSE loss of the fit. However, to train such a network would require data from a grid search in the first place. Modeling it this way would therefor be inefficient as we would only need to use the trained network once to find the optimal value of λ_{gri} and λ_{abs}. Though the trained network could have predicted values not included in the grid search, one could instead use the time needed to train the network to extend the search.

8.6 Modeling Subjects

Ideally, a bigger population of in-silco non-diabetic patients would have been used to perform the modeling of the GI extension. The BG response caused by consuming a specific food is highly individual and may vary drastically from patient to patient. Using data from a larger population would therefore ensured that a more general solution was found, better suited to model how a foods' GI effects the BG over a broad population. However, only one in-silco non-diabetic patient was available to the author at the time of writing, and thus only data from this patient was used. The proposed extension will therefor be biased towards the individual specifics of this non-diabetic patient. Additionally, a broader population of modeling subjects would have made the extension less vulnerable to errors of specific subjects, like the incorrect assumption made for the non-diabetic subject used.

As explained in section 6.4.1, data from T1DM subjects cannot be used for the modeling as these subjects will have an increased and prolonged BG response that can not be captured in the two hour time constraint of the GI calculation. It should be noted that the Basal Bolus controller included in Xie's *simglucose* [40] cannot be used to bypass this issue. This controller only considered the amount of carbohydrates in a meal when calculating the bolus dose and not the GI of these carbohydrates. It will therefor distribute the same bolus dose for meals with the same carbohydrate content, regardless of the meals GI. However, high and low GI foods cause different responses in the BG and will therefor need different amount and types of insulin to successfully control. As this is not included in the Basal Bolus controller, it cannot be used to mitigate the differences of T1DM subjects BG responses.

It was considered during the development whether the two hour time constraint could be dropped and rather the whole BG response of foods could be considered when calculating the GI. This would have allowed us to use

data from T1DM subjects for the modeling, and thereby not be so reliant on non-diabetic subjects. However, this was not possible. Our proposed extension only slows down the rate at which glucose appears in the plasma. The total amount of glucose appearing in the plasma is not changed for non-zero GI meals. Therefor, given enough time, "all" carbohydrates of a non-zero GI meal will end up as glucose in the plasma. Technically, due to f, the fraction of intestinal absorption that actually appears in plasma, only 90% of the carbohydrates will end up as glucose in the plasma. But this will be the same for all subjects. Considering the area under the curve for the whole BG response will therefore cause the recalculated GI to equal 100 for all non-zero GI meals.

8.7 Time Needed to Stabilize the Blood Glucose

The simulated postprandial BG curves illustrated in section 7.2 all depict an longer recovery time than expected, i.e. the time it takes the BG to go back to fasting levels after a meal. The literature usually depicts the BG concentrations of a standard non-diabetic person to be stable and back at fasting levels within two to four hours, as illustrated in figure 3.1. However, the response simulated for the non-diabetic showcased in 7.2 depicts a much longer recovery time. This may be due to the individual specifics of the patient as BG response is known to vary from person to person. However, the longer recovery time seen can also be explained by the incorrect assumption used for the non-diabetic patient. The parameters of this patient were modeled from mixed meal data and not glucose tolerance test data as assumed. The k_{abs} and k_{min} parameters of this patient will therefor be lower than they are assumed to be, causing longer digestion and absorption times, and herby longer effects on the BG concentrations. Since this non-diabetic patient was used to model the scaling for all other patients, these extended effects will be transmitted to the T1DM patients as well.

Part III

Food Recommendation Systems

9 Methodology

To show how the proposed GI extension can be used in the development of new diabetes treatment technologies, we will use data simulated from the extended simulator to train a food recommendation system for T1DM patients. The goal of the systems will be to recommend the optimal food to eat before exercise sessions in order to keep the BG concentrations in the normoglycemic range and avoid states of hypoglycemia. The food will be recommended in terms of amount of carbohydrates and GI. allowing the systems to choose the food with the response best suited to control a certain exercise session.

To introduce the effect exercise has on the glucose-insulin systems, Jaloli's Physical Activity model was added to our extended simulator. This was done by changing the insulin dependent utilization, $U_{id}(t)$ of the *glucose utilization subsystem* to that of equation 4.10. As no patient specific β parameter is given for the in-silco patients used, so was the median value represented in table 4.2 used instead.

9.1 Training Strategy

Similarly to meals, the BG response from exercise will be individual to each patient. To account for this, the systems must be trained on data depicting the unique response of the user. However, these systems require a lot of data to train. To collect enough data to train the systems, each user would need to

conduct several thousand exercise sessions, all with different intensities, lengths and pre-exercise meals. This is impractical as it would take years to collect all the necessary data. Additionally, for the system to perform at its optimum, it will need training samples representing all parts of the exercise spectrum, both healthy and unhealthy scenarios. Collecting this data may therefor be uncomfortable and potentially harmful to the user's health.

To work around this issue, we propose a strategy where large amounts of in-silco data are used to pre-train the systems and only small amounts of in-vivo data are used to specialize the systems to the individual users. This makes the system more user friendly as considerably less data is needed from each user. The in-silco data used to pre-train the systems will be simulated from our GI and PA extended simulator. The pre-trained systems need to be generalized in a way that makes them applicable to a broad spectrum of patients. This was done by pre-training the system on data from a large population of virtual patients.

Since no in-vivo data was available to the author at the time of writing, in-silco data from three virtual patients were used instead. These three patients were assumed to be our "real world subjects", and therefor no data from these patients were used to pre-train the systems.

9.2 Model Architecture

The food recommendation systems developed in this thesis are made from a FFNN trained to map the specific exercise scenarios to a score depicting their following BG responses. Each scenario is represented by a total of six features, describing the patient, the exercise session and the pre-exercise meal. Age and body weight are used to describe the characteristics of each patient. Carbohydrate content and GI are used to describe the meal and exercise length and intensity are used to describe exercise sessions. A score is used to depict the BG response of each scenario, summarizing the BG levels experienced throughout the scenario. This score is inspired by the reward used in reinforcement learning models.

A reward function is used to calculate the reward of each CGM measurement and the final score is set to the average reward gained in the scenario. The objective of the reward function is to depict how healthy the individual CGM measurements are, giving higher reward for measurements in the normoglycemic range and lower for those outside. As the goal of the systems is to control a patient's BG concentrations and avoid states of hypoglycemia, the asymmetric reward function depicted in Ngo et al. (2020) [6] was chosen.

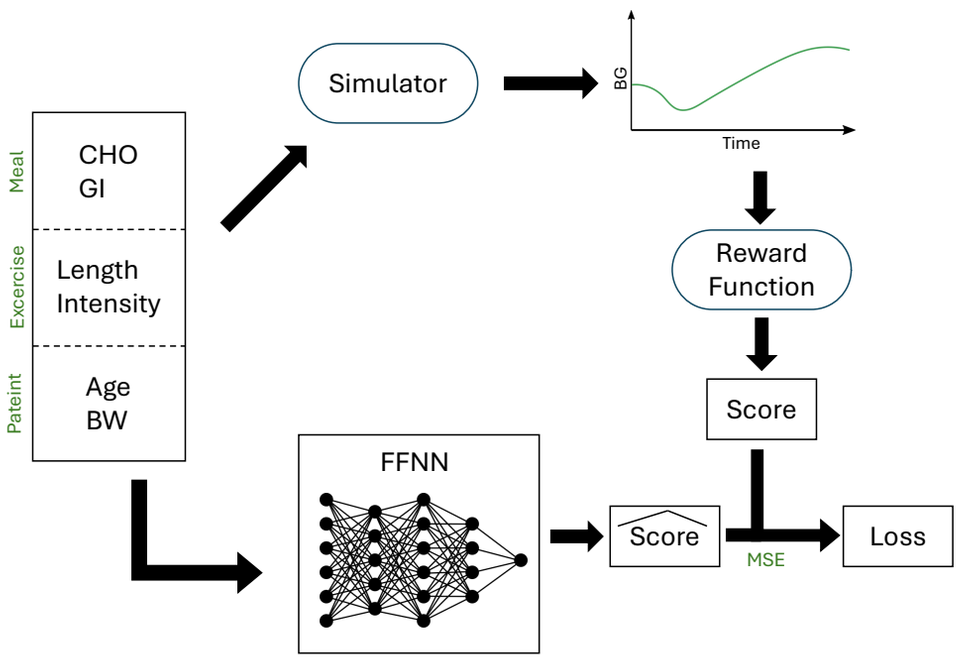

Figure 9.1: Training method for the food recommendation systems

This reward function penalizes hypoglycemic measurements more than hyperglycemic ones, thereby aligning perfectly with our intended goal. Equation 9.1 describes this reward function, where BG represent the BG measurements of the CGM.

$$r(BG) = \begin{cases} -10 & \text{if } BG < 54 \\ exp\left(\frac{ln(19.157)}{72} BG\right) - 19.157 & \text{if } 54 \leq BG < 72 \\ \frac{1}{36} BG - 2 & \text{if } 72 \leq BG < 108 \\ -\frac{1}{72} BG + \frac{5}{2} & \text{if } 108 \leq BG < 180 \\ -5 & \text{if } BG \geq 180 \end{cases} \tag{9.1}$$

The FFNNs are trained to predict this score based on the features of the scenario. The MSE loss depicted in equation 9.2 is used to evaluate the networks, measuring how the predicted score compares to the actual score of the scenarios. Figure 9.1 illustrates the whole training process where the predicted scores are depicted with a hat and the actual scores without.

$$Loss_{MSE} = \frac{1}{N_{\text{Data}}} \sum \left[\widehat{score} - score\right]^2 \tag{9.2}$$

The FFNNs used in the food recommendation systems were made up by three fully connected hidden layers with dimensions 32, 64, 16, respectively, going from the input to the output. The input layer has a dimension equal to the number of features used, and the networks have only one output, the predicted score. Each node in the hidden layers uses a ReLU activation function to introduce additional non-linearity to the model.

Once the networks were trained, they were used to find the optimal food to eat before a specific exercise session. This was done by finding the combination of carbohydrate amount and GI that resulted in the highest predicted score. The optimal food can thereby be obtained as follows:

$$CHO^*, GI^* = \underset{CHO, GI}{\operatorname{argmax}} f\big(CHO, GI \,|\, Length, Intensity, Age, BW\big), \tag{9.3}$$

where CHO^* and GI^* represent the features of the optimal food and $f(\dots)$ represent the mapping learned by the FFNN. To perform this argmax process, different combinations of CHO and GI are mapped to their predicted score $\widehat{score}$, while keeping the features representing the exercise and patient unchanged. The combination resulting in the highest score is then chosen as the optimal food for that exercise scenario.

9.3 Features and Data

The features used in the food recommendation system were chosen as they are easily obtainable by patients performing the exercise scenarios. This was done to make the system more user friendly and allow it to be trained on both in-silco and in-vivo data. By switching out the simulated BG measurement with the actual CGM measurements of a patient exercising, the same setup depicted in figure 9.1 can be used for in-vivo data.

The patient specific features Age and BW were added to help the pre-trained system specialize to the specific characteristics of the user. To represent the intensity of the exercise, the average percentage of the maximum HR was used. This was done to depict realistic average heart rates for the subjects and to make the feature space independent of the subjects age and body weight. The intensity of the exercise will then be given by equation 9.4:

$$Intensity = \frac{\overline{HR}}{HR_{max}}, \tag{9.4}$$

where $\overline{HR}$ is the average HR of the exercise session and HR_{max} is the subjects maximum heart rate.

Name	ID	Age	BW [kg]
adult#001	1	61	102.32
adult#002	2	65	111.10
adult#003	3	27	81.63
adult#004	42	66	63.00
adult#005	5	52	94.07
adult#006	6	26	66.10
adult#007	7	35	91.23
adult#008	8	48	102.79
adult#009	9	68	74.60
adult#010	10	68	73.86
adult#011	51	24	76.37
adult#012	52	27	102.62
adult#013	53	70	74.61
adult#014	54	62	57.32
adult#015	55	40	59.06
adult#016	56	77	68.71
adult#017	57	23	97.32
adult#018	58	47	68.28
adult#019	59	44	64.00
adult#020	60	66	66.63

Table 9.1: Virtual patient population.

9.4 Data Production

The data used to train the food recommendation systems was produced through repeated simulations of the extended simulator. The virtual patient population was extended beyond that of the 10 adult T1DM patients included in Xie's *simglucose* [40] by adding the 10 adult T1DM patients listed in the US patent for the 2008 version of the UVA/Padova simulator [49]. Similarly to the case of adding the non-diabetic patient, not all parameters required by *simglucose* were included in the patent. The missing parameters were calculated using the basal states equation listed in [7; 1; 36; 50]. The new virtual patient population is described in table 9.1 where adult#011 to adult#020 are the added patients.

This new virtual patient population was split into three sub populations with similar average body weight and age. The split was done based on the intended use-cases, training, test and validation (see table 9.2 to 9.3). Data from the fourteen patients in the training population was used to pre-train the food recommendation systems. Data from the three patients included in the test population was used to test the food recommendation systems under pre-

Name	ID	Age	BW [kg]
adult#002	2	65	111.10
adult#004	42	66	63.00
adult#006	6	26	66.10
adult#007	7	35	91.23
adult#008	8	48	102.79
adult#009	9	68	74.60
adult#010	10	68	73.86
adult#012	52	27	102.62
adult#013	53	70	74.61
adult#014	54	62	57.32
adult#015	55	40	59.06
adult#016	56	77	68.71
adult#017	57	23	97.32
adult#019	59	44	64.00

Table 9.2: Training population.

Name	ID	Age	BW [kg]
adult#005	5	52	94.07
adult#011	51	24	76.37
adult#020	60	66	66.63

Table 9.3: Test population.

training. The three patients of the valuation population were used as our three "real life" subjects.

To produce the training and test data sets used for to pre-train the model, a total of 2048 simulations were conducted for each patient in the training and test population. This results in a training set of 2048×14 data points and a test set of 2048×3 data points. Only 105 simulations were conducted for each the patients in the validation population, resulting in three training data sets of 105 data points each. No test data was used for the validation subjects.

Simulations were conducted for each patient on a variety of different exercise

Name	ID	Age	BW [kg]
adult#001	1	61	102.32
adult#003	3	27	81.63
adult#018	58	47	68.28

Table 9.4: Validation population.

sessions and pre-exercise meals. The data sets were produced by recording the different features used in the simulated scenarios together with the score of each scenario. The *Age* and *BW* feature was determined by the specific virtual patient used, while the other features were sampled randomly from the following ranges:

$$CHO \in [0.0,\ 75.0]\ \text{g}, \qquad GI \in [0,\ 100], \tag{9.5}$$

$$Length \in [15.0,\ 120.0]\ \text{min}, \qquad Intensity \in [0.5,\ 0.85]. \tag{9.6}$$

To ensure coverage from all parts of the feature space while keeping the data sets relatively small, each feature range was split into smaller sub-ranges. Different combinations of these sub-ranges were used for each simulation. The exact features used for each simulation were then sampled uniformly from their respective sub-ranges. This technique was used for all the virtual patients, ensuring an unbiased dataset with similar coverage for all patients.

All simulated scenarios were made up by a exercise session and a pre-exercise meal. The exercise session starts 30 minutes after the start of the simulation and lasts for 15 to 120 minutes. The patients start consuming the pre-exercise meal 15 minutes before the exercise at a rate of 5g CHO per minute. Each patient is administrated a patient specific basal dose during the simulation to ensure steady fasting BG levels. No bolus doses were administrated. The Basal-Bolus controller included in Xie's *simglucose* is used to calculate these doses. All patients are assumed to have a resting HR of 72 bpm to comply with the average resting HR of our age groups [51], and the patients maximum HRs were assumed to follow the commonly used Age-Predicted Maximum Heart Rate (APMHR) formula:

$$HR_{max} = 220\,bpm - Age\,, \tag{9.7}$$

introduced by Fox et al. (1971) [52]. The patient specific β parameter is set to its median value of 0.0446 for all patients. All scenarios are simulated until 8 hours after the end of the exercise to ensure a good depiction of the post exercise BG response. All simulations of a patient were done with the same simulation seed. However, different seeds were used for each individual patient.

10

Experiment: The Impact of Knowing Foods Glycemic Index

A small experiment was conducted to determine the impact knowing a food's GI has on food recommendation systems under the premises of the proposed extension. Two sets of three food recommendation systems were trained, two for each our "real" patients included in table 9.4. The first set was trained using GI as one of the input features to the FFNN, and the second without this feature, thereby only describing the pre-exercise meals in terms of their carbohydrate amounts. Both sets of food recommendation systems otherwise had the exact same architecture as described in section 9.2 and were trained on the same set of simulated data with the same training setup.

10.1 Evaluation Metrics

To evaluate the recommendations of the systems, the exercise scenarios will be re-simulated with their recommended pre-exercise meals. CGM data from the re-simulated scenarios will then be used to calculate score and TIR metrics for each recommendation. The same setup and patient-specific simulation seed as used when producing the original data will be used to re-simulate the optimal

meal scenarios. The score metric is calculated the same way as for the original simulated data, using the same reward function. Equation 10.1 summarizes this metric, where $r(\dots)$ is the reward function, CGM_t are the different CGM measurements of the scenario, and T is the total number of measurements in the scenario.

$$Score = \frac{\sum_{t=0}^{T} r(CGM_t)}{T} \tag{10.1}$$

The second metric used is the Time In Range (TIR). This metric depicts the portion of time the CGM measurements were in the normoglycemic range during the scenario as summarized by equation 10.2.

$$TIR = \frac{\#\, CGM_t \in [70,\ 180]\ \text{mg/dl}}{T} \tag{10.2}$$

11

Results

In this section, we will build on the proposed methodology of section 9 and depict the results of the food recommendation systems. Section 11.2 will present the result of the systems trained with the knowledge of the foods GI, hereby referred to as the GI models, and section 11.3 will present the results of the systems trained without this knowledge, hereby referred as the non-GI models. The final section of this chapter will look at some examples of how these models controls the patients BG during a exercise scenario.

11.1 Training Process

The food recommendation systems presented in this chapter were all trained using the architecture and training strategy described in section 9. The systems were pre-trained on the data simulated from the 14 virtual patient included in table 9.2 for a total of 28672 training samples. A test set of 6174 data samples simulated from the test population was used during the pre-training process, along with a dropout rate of 0.1. This was done to make the pre-trained system more generalized to non-seen patients, and avoid overfitting the training data. The systems were pre-trained for 1000 epochs using an Adam optimizer with a learning rate of 10^{-4} and a weight decay (L2 term) of 10^{-2} on small batches with 10 samples per batch.

Two pre-trained systems were made, one for the GI models qhich use the GI of

the pre-exercise meals as a feature, and one for the non-GI models which do not use the GI as feature. Once the systems were pre-trained, specialized versions of them were trained for each of the patients in table 9.4. The specialized systems were trained on 105 data samples simulated from their respective patients. No test data or dropout rate was used during this training process as we want the system to be specific to each patient. Each specialized version was trained for 1000 epochs, using the same optimizer and hyper-parameters as the pre-trained systems.

Once the patient specific systems were trained, they were used to recommend the optimal pre-exercise meal for the patients. This was done through equation 9.3 where only meals with features in the following intervale were considered:

$$CHO \in [0, 1, 2, 3, 4, \ldots, 100] \qquad GI \in [0, 1, 2, 3, 4, \ldots 100]. \tag{11.1}$$

11.2 With Glycemic index

In this section, we present the recommendations made by the patient specific food recommendation systems trained with the knowledge of a food's GI. Table 11.1 depicts some of the pre-exercise meals recommended by the GI models for each of our validation patients. The recommendations depicted are made for exercise session with lengths between 30 to 120 minutes and intensities of 0.55 to 0.85. The table at the top shows the meals recommended for adult#001, the one in the middle shows the meals recommended for adult#003, and the one at bottom shows the meals recommended for adult#018. The recommended meals are depicted in terms of both carbohydrate amounts and GI.

We can see that both the carbohydrate amounts and the GI of the meals recommended for each patient steadily increases with the length and intensities of the exercise sessions. This makes sense as longer and more intense exercises would cause more drastic effects on the BG concentration than shorter less intense exercises. Additionally, it is worth noting that the recommended meals for adult#018 are on average smaller than those for the other two patients.

Table 11.2 shows the score and TIR metrics for each of the recommendations made by the patient-specific GI models in table 11.1.

adult#001 GI Model		Length [min]							
		30.0		60.0		90.0		120.0	
		CHO	GI	CHO	GI	CHO	GI	CHO	GI
Intensity [%HR_{max}]	0.55	0.0	0.0	0.0	0.0	0.0	0.0	0.0	0.0
	0.65	0.0	0.0	6.0	38.0	8.0	41.0	18.0	43.0
	0.75	0.0	0.0	7.0	38.0	36.0	100.0	54.0	100.0
	0.85	0.0	0.0	9.0	38.0	48.0	100.0	60.0	100.0

adult#003 GI Model		Length [min]							
		30.0		60.0		90.0		120.0	
		CHO	GI	CHO	GI	CHO	GI	CHO	GI
Intensity [%HR_{max}]	0.55	0.0	0.0	0.0	0.0	5.0	4.0	21.0	100.0
	0.65	0.0	0.0	4.0	32.0	26.0	100.0	24.0	100.0
	0.75	0.0	0.0	26.0	96.0	35.0	100.0	45.0	100.0
	0.85	1.0	37.0	29.0	100.0	36.0	100.0	46.0	100.0

adult#018 GI Model		Length [min]							
		30.0		60.0		90.0		120.0	
		CHO	GI	CHO	GI	CHO	GI	CHO	GI
Intensity [%HR_{max}]	0.55	0.0	0.0	0.0	0.0	0.0	0.0	0.0	0.0
	0.65	0.0	0.0	0.0	0.0	1.0	100.0	0.0	0.0
	0.75	0.0	0.0	0.0	0.0	15.0	100.0	31.0	85.0
	0.85	0.0	0.0	11.0	100.0	26.0	100.0	39.0	100.0

Table 11.1: The GI models optimal pre-exercise meal recommendations for exercise sessions of length 30 min, 60 min, 90 min and 120 minutes, with intensities 55%, 65%, 75% and 85% of maximum HR. The top table shows the recommendation results for adult#001, the middle table shows the results for adult#003 and the bottom table shows the results for adult#018.

adult#001 GI Model		Length [min]							
		30.0		60.0		90.0		120.0	
		Score	TIR	Score	TIR	Score	TIR	Score	TIR
Intensity [%HR_{max}]	**0.55**	0.640	1.000	0.679	1.000	0.706	1.000	0.734	1.000
	0.65	0.690	1.000	0.699	1.000	0.687	1.000	0.660	1.000
	0.75	0.724	1.000	0.665	1.000	0.556	1.000	0.513	1.000
	0.85	0.701	1.000	0.256	0.942	0.473	0.990	0.400	0.976

adult#003 GI Model		Length [min]							
		30.0		60.0		90.0		120.0	
		Score	TIR	Score	TIR	Score	TIR	Score	TIR
Intensity [%HR_{max}]	**0.55**	0.605	1.000	0.692	1.000	0.606	1.000	0.532	1.000
	0.65	0.693	1.000	0.602	1.000	0.473	1.000	0.301	0.957
	0.75	0.691	1.000	0.449	1.000	0.192	0.955	-0.189	0.915
	0.85	0.583	0.994	0.044	0.937	-0.622	0.876	-0.992	0.844

adult#018 GI Model		Length [min]							
		30.0		60.0		90.0		120.0	
		Score	TIR	Score	TIR	Score	TIR	Score	TIR
Intensity [%HR_{max}]	**0.55**	0.516	1.000	0.601	1.000	0.671	1.000	0.725	1.000
	0.65	0.587	1.000	0.719	1.000	0.733	1.000	0.656	1.000
	0.75	0.666	1.000	0.715	1.000	0.668	1.000	0.608	1.000
	0.85	0.721	1.000	0.657	1.000	0.306	0.945	0.299	0.948

Table 11.2: Evaluation criteria results, score and TIR, of the GI models optimal pre-exercise meal recommendations for exercise sessions with length 30 min, 60 min, 90 min and 120 minutes, with intensities 55%, 65%, 75% and 85% of maximum HR. The top table shows the criteria results for adult#001, the middle table shows the results for adult#003, and the bottom table shows the result for adult#018.

11.3 Without Glycemic index

In this section, we present the recommendations made by the patient-specific food recommendation systems trained without the knowledge of a food's GI. Table 11.3 shows the pre-exercise meals recommended by the non-GI models for each of the validation patients on the same set of exercise scenarios as the recommendations depicted for the GI models. The recommendations for adult#001 are shown at the top, the ones for the adult#003 are shown in the middle, and the ones for adult#018 are shown at the bottom. The pre-exercise meals are only recommended in terms of their carbohydrate content as GI is not included in these models.

Though these systems were trained without knowing the pre-exercise meal's GI, we can see that they were able to learn the connection between the amount of carbohydrates in a meal and the effect it has on the patients' BG concentrations. Similarly to the GI models, the carbohydrate amount recommended by the non-GI increases as the length and intensities of the exercise sessions increases. We can however see some inconsistencies in the recommendations, as the non-GI model for adult#003 recommends to eat less for the 120 min than for the 60 and 90 min sessions with medium high intensities.

Table 11.4 shows the score and TIR metrics for the recommended pre-exercise meals of the non-GI models. As these models only recommend the carbohydrate content, and have no knowledge of the meals GI, each recommended meal was assigned a random GI when re-simulated. This was done to represent the uncertainty surrounding the GI of pre-exercise meals consumed by patients following these recommendations. This uncertainty will affect the evaluation metrics of these systems.

11.4 Comparison

This section will compare the recommendations made by the GI models and non-GI models. The average score and TIR metrics of the recommendations made for each patient are depicted in table 11.5 as well as the average metrics across all patients. Only the exercise scenarios included in table 11.1 and 11.3 are considered towards the average metrics.

The average metrics for the GI models are consistently higher or equal to those for the non-GI models. This does indicate that knowing a meals GI has a positive impact on food recommendation systems under the premise of our proposed extension. Though the average metrics for the non-GI model are lower than the ones for the GI models, they still depict a good result with an

adult#001 Non-GI Model		**Length** [min]			
		30.0	**60.0**	**90.0**	**120.0**
		CHO	**CHO**	**CHO**	**CHO**
Intensity [%HR_{max}]	**0.55**	0.0	0.0	0.0	9.0
	0.65	0.0	0.0	5.0	25.0
	0.75	0.0	8.0	36.0	43.0
	0.85	0.0	26.0	40.0	66.0

adult#003 Non-GI Model		**Length** [min]			
		30.0	**60.0**	**90.0**	**120.0**
		CHO	**CHO**	**CHO**	**CHO**
Intensity [%HR_{max}]	**0.55**	0.0	0.0	0.0	16.0
	0.65	0.0	3.0	25.0	18.0
	0.75	0.0	26.0	25.0	18.0
	0.85	9.0	27.0	25.0	24.0

adult#018 Non-GI Model		**Length** [min]			
		30.0	**60.0**	**90.0**	**120.0**
		CHO	**CHO**	**CHO**	**CHO**
Intensity [%HR_{max}]	**0.55**	0.0	0.0	0.0	0.0
	0.65	0.0	0.0	19.0	23.0
	0.75	0.0	4.0	23.0	28.0
	0.85	0.0	12.0	32.0	43.0

Table 11.3: The non-GI models optimal pre-exercise meal recommendations for exercise sessions of length 30 min, 60 min, 90 min and 120 minutes, with intensities 55%, 65%, 75% and 85% of maximum HR. The top table shows the recommendation results for adult#001, the middle table shows the results for adult#003 and the bottom table shows the results for adult#018.

adult#001 Non-GI Model		Length [min]							
		30.0		60.0		90.0		120.0	
		Score	TIR	Score	TIR	Score	TIR	Score	TIR
Intensity [%HR_{max}]	**0.55**	0.640	1.000	0.679	1.000	0.706	1.000	0.689	1.000
	0.65	0.690	1.000	0.723	1.000	0.698	1.000	0.625	1.000
	0.75	0.724	1.000	0.658	1.000	0.547	1.000	0.163	0.915
	0.85	0.701	1.000	0.570	1.000	0.028	0.915	-0.648	0.858

adult#003 Non-GI Model		Length [min]							
		30.0		60.0		90.0		120.0	
		Score	TIR	Score	TIR	Score	TIR	Score	TIR
Intensity [%HR_{max}]	**0.55**	0.605	1.000	0.692	1.000	0.627	1.000	0.504	1.000
	0.65	0.693	1.000	0.605	1.000	0.442	1.000	0.139	0.929
	0.75	0.691	1.000	0.227	0.948	-0.518	0.876	-1.148	0.806
	0.85	0.577	0.989	-0.248	0.911	-1.244	0.816	-1.449	0.787

adult#018 Non-GI Model		Length [min]							
		30.0		60.0		90.0		120.0	
		Score	TIR	Score	TIR	Score	TIR	Score	TIR
Intensity [%HR_{max}]	**0.55**	0.516	1.000	0.601	1.000	0.671	1.000	0.725	1.000
	0.65	0.587	1.000	0.719	1.000	0.578	1.000	0.632	1.000
	0.75	0.666	1.000	0.705	1.000	0.612	1.000	0.605	1.000
	0.85	0.721	1.000	0.641	1.000	0.144	0.935	0.327	0.953

Table 11.4: Evaluation criteria results, score and TIR, of the non-GI models optimal pre-exercise meal recommendations for exercise sessions with length 30 min, 60 min, 90 min and 120 minutes, with intensities 55%, 65%, 75% and 85% of maximum HR. The top table shows the criteria results for adult#001, the middle table shows the results for adult#003, and the bottom table shows the result for adult#018.

Comparison	adult#001		adult#003		adult#018		Total	
	Score	TIR	Score	TIR	Score	TIR	Score	TIR
GI Model	0.611	0.994	0.291	0.967	0.616	0.993	0.506	0.985
Non-GI Model	0.512	0.981	0.075	0.941	0.591	0.993	0.392	0.972

Table 11.5: The average score and TIR of the GI modles and non-GI models optimal pre-exercise meal recommendations, for adult#001, adult#003, adult#018 and overall.

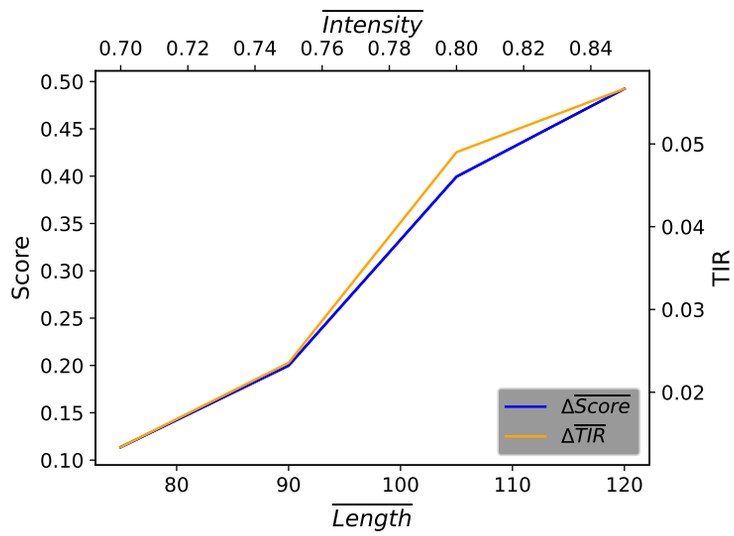

Figure 11.1: The trend of the difference in average score (blue line) and average TIR (orange line) metrics, of the GI and non-GI models, as the average intensity and length of the exercise sessions increases. The top x-axis shows the average intensities of the exercise sessions, and the bottom shows the average length. The difference in average Score is depicted by the y-axis on the left, and the average difference in TIR is depicted on the right.

average *TIR* score of over 90% for all patients. A trend can be seen between the length and intensity of an exercise scenario and the difference in the score and TIR metrics between the models. Longer and more intense exercise scenarios reflect lower metrics than the shorter and less intense scenarios. This is the case for both set of models. However, this trend is steeper for the non-GI models than for the GI models. Figure 11.1 illustrates this by depicting the difference between the average metrics of the models (GI model − non-GI model) as the average intensity and length of the considers exercise sessions increases.

11.4.1 Recommendations of Different Optimality

In addition to returning the pre-exercise meal the systems consider optimal for a specific exercise session, the systems are capable of returning the meals they consider non-optimal as well. This can be of interest when judging if the systems has learned the desired aspects of the task.

In this section, we will look at three of the scenarios depicted in the tables above, one for each of our validation patients, and compare the optimal, sub-

Exercise Scenarios	adult#001	adult#003	adult#018
Length [min]	90.0	60.0	120.0
Intensity [%HR_{max}]	0.75	0.85	0.65

Table 11.6: The exercise scenarios examined for each patient.

GI-Model	adult#001		adult#003		adult#018	
	CHO	GI	CHO	GI	CHO	GI
100% Optimal	36	100	29	100	0	0
50% Optimal	13	16	54	26	50	44
0% Optimal	100	60	100	17	100	100

Table 11.7: The GI models 100% optimal, 50% optimal and 0% optimal pre-exercise meal recommendations for each of the patient specific exercise scenarios examined.

optimal and non-optimal recommended meals of the different models. The optimal meals of the scenarios will be the ones depicted in tables 11.1 and 11.3. The suboptimal meals will be the ones the systems consider to be 50% optimal for the considered scenario. And the non-optimal meals will be the ones considered to be 0% optimal, in other words, the worst pre-exercise meal to eat in the considered exercise scenarios. Only features in the ranges depicted in equation 11.1 are considered when determining the optimal, sub-optimal and non-optimal meals. So even though a meal containing more then 100 grams carbohydrates may be worse, these will not be considered by the systems.

The lengths and intensities of the three exercise scenarios examined are summarized in table 11.6. Tables 11.7 and 11.8 show the optimal, sub-optimal and non-optimal pre-exercise meals recommended by the models for each scenarios. Figure 11.2 to 11.4 depict the re-simulated BG curves each of these scenarios. The same re-simulation process as used to produce the evaluation metrics was also used here, using the same simulation seed and randomly assigned GI per exercise scenario.

Non-GI-Model	adult#001	adult#003	adult#018
	CHO	CHO	CHO
100% Optimal	36	27	23
50% Optimal	3	50	50
0% Optimal	100	100	70

Table 11.8: The non-GI models 100% optimal, 50% optimal and 0% optimal pre-exercise meal recommendations for each of the patient specific exercise scenarios examined.

Table 11.7 and 11.8 show a similar trend in the carbohydrate content of the recommended meals. It becomes evident from the BG curves illustrated in figures 11.2 to 11.4 that both systems have managed to learned the essence of the task. Following the optimal recommendations is in each scenario shown to best control the patients BG concentrations. This is the case for both models' recommendations. The only possible exception would be for the first scenario where following the non-GI model's optimal meal recommendation seems to cause an increase in the BG concentrations towards the end of the scenario. This may be due to the random GI of the meal and depending on the duration of the increase, following the sub-optimal recommendation could be a healthier choice here.

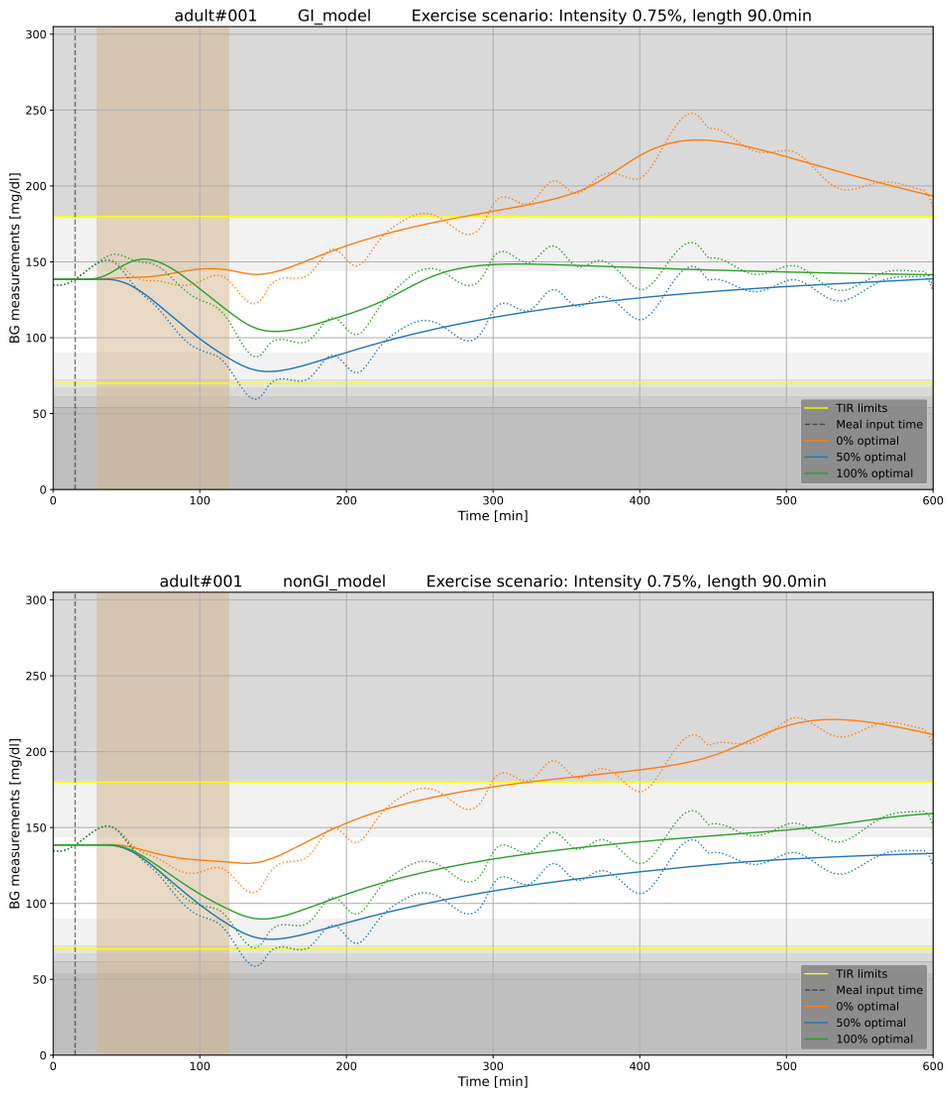

Figure 11.2: The BG curves for exercise scenario; intensity 75%, length 90.0 min for adult#001, following the 100% optimal (green curve), 50% optimal (blue curve) and 0% optimal recommendations from the GI model (upper plot) and the Non-GI model (lower plot). The solid curves shows the subcutaneous glucose values while the dotted curves shows the CGM values. The timing of the exercise session is marked in beige, and the consumption time of the pre-exercise meal is depicted by vertical dashed line. The limits of the TIR interval are marked by the horizontal yellow lines, and the different shades of gray represent the associated rewards, the darker the shade the worse reward.

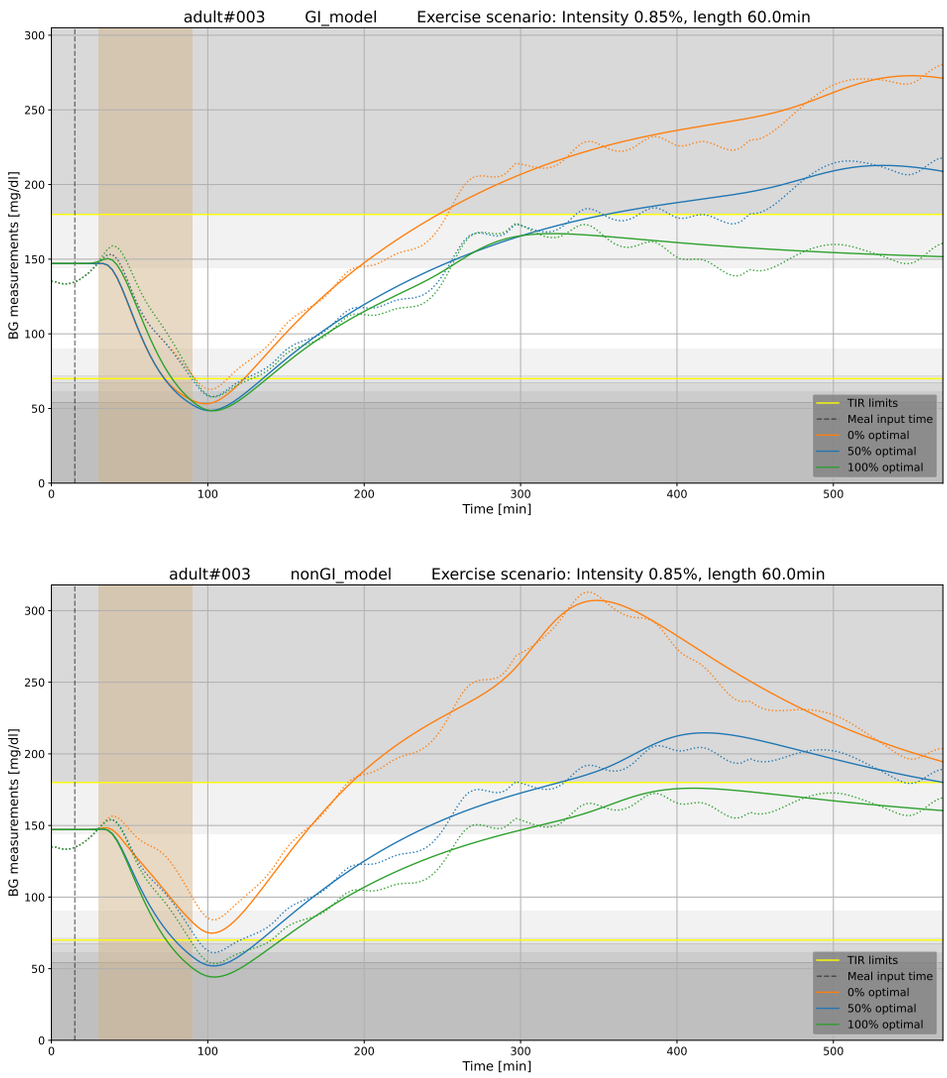

Figure 11.3: The BG curves for exercise scenario; intensity 85%, length 60.0 min for adult#003, following the 100% optimal (green curve), 50% optimal (blue curve) and 0% optimal recommendations from the GI model (upper plot) and the Non-GI model (lower plot). The solid curves shows the subcutaneous glucose values while the dotted curves shows the CGM values. The timing of the exercise session is marked in beige, and the consumption time of the pre-exercise meal is depicted by vertical dashed line. The limits of the TIR interval are marked by the horizontal yellow lines, and the different shades of gray represent the associated rewards, the darker the shade the worse reward.

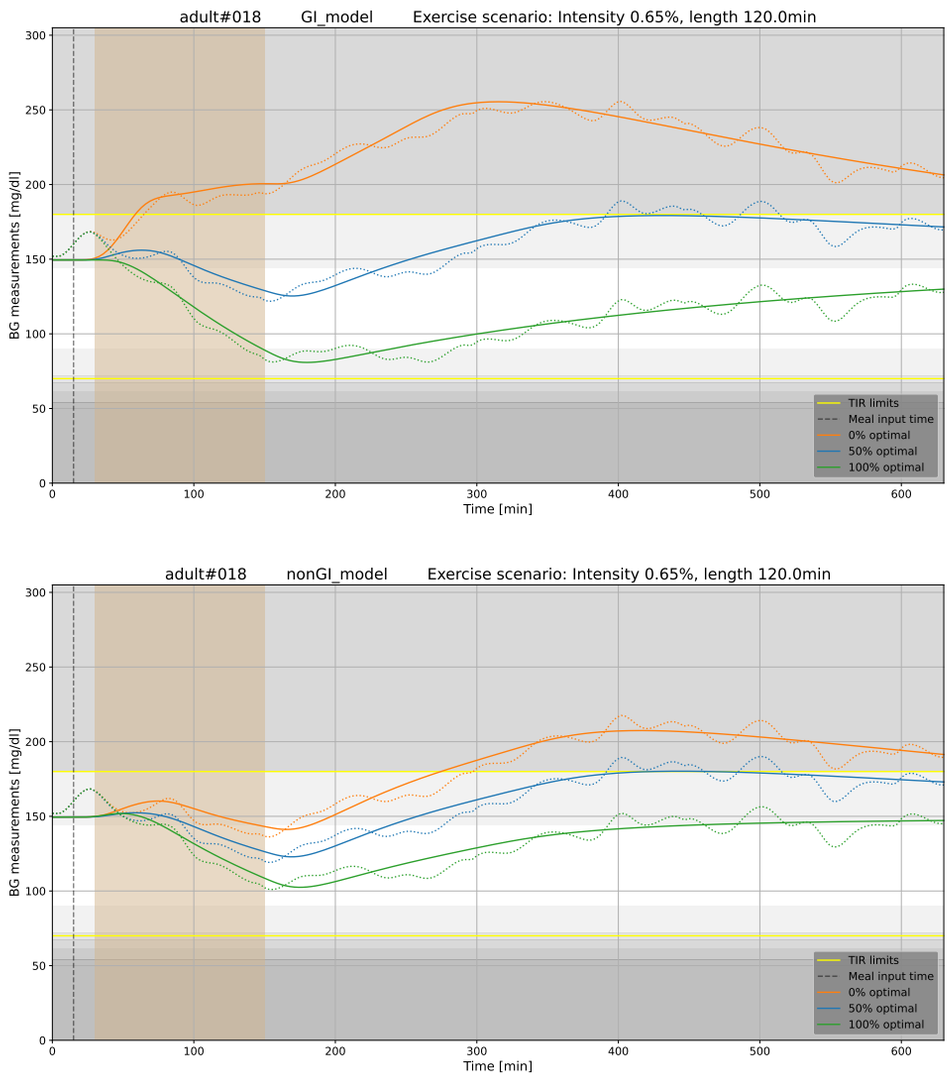

Figure 11.4: The BG curves for exercise scenario; intensity 65%, length 120.0 min for adult#018, following the 100% optimal (green curve), 50% optimal (blue curve) and 0% optimal recommendations from the GI model (upper plot) and the Non-GI model (lower plot). The solid curves shows the subcutaneous glucose values while the dotted curves shows the CGM values. The timing of the exercise session is marked in beige, and the consumption time of the pre-exercise meal is depicted by vertical dashed line. The limits of the TIR interval are marked by the horizontal yellow lines, and the different shades of gray represent the associated rewards, the darker the shade the worse reward.

12 Discussion

In this section we will discuss the methodology and results for the food recommendation models trained in this thesis.

12.1 Practicality of the Systems

The features and training strategy used for the food recommendation systems proposed in this thesis were chosen to make the systems easily practical to train and use in real world scenarios. The data required to train the systems can be collected by the users perform exercise scenarios while monitoring their BG concentrations and average HR of the session. T1DM patients equipped with a CGM sensor will have easy access to their BG measurements during the scenario and a modern fitness watch may be used to measure the average HR as well as the length of an exercise session. The features of the pre-exercise meal can be found in the food's listed nutritional content, or looked up in international tables [35]. Including the patients age and body weight as features enables the systems to adapt to dynamic changes in the patients state, and thereby allowing them to be used for a longer duration before needing to be re-trained.

The systems trained in this thesis were trained on data from 105 simulated training scenarios per patient. Though this is nowhere close to the amount of data used to pre-train the model, but it is still a large amount. A standard patient training twice a week would have to use a whole year to collect enough

data to train these models. Ideally, the amount of data needed to specialize these systems to a specific patient would be lowered to allow the systems to be used in a quicker time frame. Additionally, to make the systems more robust to exercise scenarios not included in the training data, some of the user collected data should be used to test the systems under training. Pre-training the systems on a bigger virtual patient population could help lower the amount of data needed to specialize them by making the pre-trained systems more generalized to the different characteristics of each user. The virtual patient population was expanded from 10 to 20 T1DM patient for this reason as well as to make the resulting population less biased towards older and heavier patients as 6 out of 10 patients included in Xie's *simglucose* [40] are over the age of 50, and 5 out of 10 weigh above 90 kg. No other virtual patients than those depicted in table 9.1 were available to the author at the time of writing.

12.2 The Chosen Architecture

The food recommendation models proposed in this thesis use a FFNN to learn the mapping from a set of features describing the exercise scenarios to a score summarizing the BG levels of the scenarios. This learned mapping is then used to find the pre-exercise meal resulting in the highest predicted score. It is however possible to use the simulator directly to find these optimal pre-exercise meals by using the actual score of the simulations instead of the networks predicted score. However, this would be significantly slower as each meal scenario can take up to one minute or more to simulate while a forward pass through the trained networks will only take a couple of seconds at max. As 101×101 different meals are tested per scenario, it would be considerably more time consuming and impractical to the user to use the simulator directly than to use the trained networks. Additionally, to be able to use the simulator, the patients must first get a virtual representation made of themselves. Performing the trials needed to model the parameters of the simulator would be more expensive and require more data from each patient than to train the food recommendation systems.

12.3 Length and Intensity's effect on the Recommendations

The exercise sessions were described in terms of length and intensity as these are the two main factors determining the effect exercise has on the BG concentrations. Exercising at higher intensity will cause the BG concentrations to

decrease faster than lower intensities and the length of the session determines the duration of the decrease. One would assume that high GI food would therefore be a good choice for short and intense exercises as these foods cause a quick, short-lived response in the BG concentrations, thereby counteracting the effect of the exercise. Following the same logic, one would also assume that lower GI food would be more ideal for long exercise sessions of less intensity as these would counteract the effect of the long exercise.

It is therefor interesting that few low GI meals where recommended in the longer sessions considered, as these would technically have a longer lasting effect suited for these scenarios. However, when considering the extended response of these meals depicted in figure 7.3, it becomes evident that a 120 session is too short of a time frame to effectively utilize this effect. A meal with a low GI would likely keep affecting a patient's BG levels long after the end of the exercise session considered and may therefore cause states of hyperglycemia. This is also the reason why high GI meals are recommended so often by the systems as these foods would have a shorter effect on the BG concentrations and are more suited to the short lengths considered.

12.4 The Reward Functions effect on the Recommendations

The BG levels corresponding to the maximum reward for the reward function used is 108 mg/dL. This is significantly lower than the fasting BG levels of our validation patients which are around 150 mg/dL. This will cause the food recommendation systems to favor scenarios where the BG levels are slightly lowered from the fasting levels as these will result in a higher score. This can be seen in figure 11.4, where the optimal curve of the GI model are shown to diverge more from the fasting levels than the sub-optimal curve. This can also be seen in the number of exercise scenarios where the systems recommend no meal to be eaten as small decreases to the BG concentrations are considered to be more optimal than staying at the fasting levels. However, this bias towards scenarios that slightly decreases the patients BG concentration is not a bad thing. As T1DM have chronically high BG levels, both fasting and non-fasting, lowering them to the optimal value of around 108 mg/dL would only improve a patient's health.

12.5 Age and Body Weight's effect on the Recommendations

A connection was found between the age and BW of a patient and the food required to control their BG concentrations during exercise sessions. The less body weight a patient has, the less food they need to keep the BG concentrations stable during the exercise. This is represented in the original *glucose rate of appearance subsystem* as the rate of appearance, Ra, is scaled by a factor of $\frac{1}{BW}$, thereby causing patients with less BW to be more affected by their consumed carbohydrates and will therefor need less food than patients of higher BW.

Additionally, older patients usually have a lower maximum HR than younger patients. This is assumed to be the case for our patients as we follow the APMHR depicted in equation 9.7 to calculate our patients maximum HR. This means that a young and an old patient exercising at the same intensity would have different average HRs during the session. In particular, the young patient would have a higher average HR than the old patient. The change in HR, $\Delta HR = \overline{HR} - HR_b$, would also be different for the two patients as we assume all patients have the same resting HR of $HR_b = 72\,\text{bpm}$. The PA extensions models the effect exercise has on the glucose-insulin systems solely based on this change in HR, thus causing the young patient to be more affected by the exercise than the old patient.

So, the older a patient is and the less BW they have, the less food is required to control their BG concentration during the exercise scenarios, while younger and heavier patients will require more food to control their BG concentrations during the exercise. This can be seen in the pre-exercise meals recommended for adult#018 as these are on average smaller then the ones recommended for two other validation patients.

The assumptions for the resting and maximum HR were made as no patient-specific HR_b or HR_{max} values were included for the virtual patients used. In real world cases, should these values ideally be implemented by the users, if viable, to better depict there individual response to exercise.

12.6 Experiment and exercise scenarios

The experiment conducted depicts similar results for both food recommendation systems trained with and without the knowledge of foods GI. The evaluation metrics of the GI models are on average higher for the considered

exercise scenarios than those for the non-GI models, but not by a big margin. This would indicate that the impact of knowing a food's GI is smaller than previously thought. However, as evident by the trend in figure 11.1, this is more likely an effect of the considered set of exercise scenarios used to evaluate the models. A bigger set of exercise scenarios including longer and more intense sessions would likely be better suited to depict the differences, and the impact knowing a food's GI has on these models. Due to the amount of low intensity and short exercise sessions considered and the reward functions bias towards decreasing the BG concentration, patients are recommended to eat no pre-exercise meal in almost half of the evaluated scenarios. Both systems will have exactly the same score and TIR metrics for these no food scenarios. Due to the amount of them considered, this will lower the total impact of the scenarios where the meal's GI actually matters for the recommendation.

Part IV

Conclusion

13

Summary and Conclusion

In the first half of this thesis, a proposed extension to the UVA/Padova BG simulator was presented, adding the effect a food's GI has on the glucose-insulin system. The ability to depict meals both in terms of carbohydrate content and GI will allow for more nuanced and realistic simulations of patient's postprandial BG responses. The availability of a simulation model capable of this will therefor be beneficial to the development of food recommendation systems.

Due to the lack of available in-vivo data, the extension was modeled on in-silco data by fitting the GI depicted by the simulated postprandial BG levels to the GI of the simulated meals. Only in-silco data from non-diabetic patients were suitable to perform this modeling due to the time constraint of the GI calculations. This severely limits the number of available modeling subjects.

Though lacking sufficient modeling data, the modeled extension shows promising results with a MSE of 1.380 between the simulated and recalculated GI of the modeling subjects and the simulations correctly capture the effect a food's GI has on the BG response as described in the literature for both non-diabetic and T1DM patients. Further research and sufficient in-vivo data is however required to evaluate the accuracy of this extension. It is therefor difficult to draw a conclusion based on the present results. Nonetheless, the extensions ability to depict the characteristic effect the GI has on the BG concentrations should still be admired as it proves the possibility of this type of extension. We therefor hope our model can work proof of concept and as a baseline for

further research in the field.

The second half of this thesis focused on how the proposed GI extension could be used in the development of food recommendation systems. Regular exercise is an important part of the diabetes treatment. However, many T1DM are prone to experience states of hypoglycemia during exercise sessions. This may be unpleasant for the patients and may cause them to develop a restraint towards exercising. The availability of food recommendation systems that can recommend the optimal meal to control a patient's BG concentrations during exercise and avoid hypoglycemic states is therefore crucial. Utilizing both the carbohydrate content and GI of meals will theoretically allow the systems to be used in a wider range of exercise scenarios.

A small experiment was conducted to determine the effect of using GI as a feature of food recommendation models trained to recommend the optimal pre-exercise meals. Food recommendation systems both with and without the knowledge of meals GI were trained, using a strategy of pre-training the systems on large amount of in-silco data to lower the required data needed to apply the systems to real life scenarios. The results of the experiment depict a small positive impact of using GI knowledge on the set of exercise scenarios considered. However, it can be seen that the impact of using GI grows as the length and intensity of the considered sessions increases, thereby aligning with our initial expectations.

Bibliography

[1] Chiara Dalla Man, Marc D. Breton, and Claudio Cobelli. Physical activity into the meal glucose—insulin model of type 1 diabetes:in silicostudies. *Journal of Diabetes Science and Technology*, 3(1):56–67, January 2009.

[2] Ngo P. & Tayefi M. & Nordsletta A.T. & Godtliebsen F. Food recommendation using machine learning for physical activities in patients with type 1 diabetes. pages Page 1–5, 2019.

[3] American Diabetes Association understanding and managing low blood glucose (hypoglycemia)). `https://diabetes.org/living-with-diabetes/treatment-care/hypoglycemia`. Accessed: September 19, 2024.

[4] Claudia Cecilia Yamamoto Noguchi, Shogo Hashimoto, and Eiko Furutani. *in silico* blood glucose control for type 1 diabetes with meal announcement using carbohydrate intake and glycemic index. *Adv. Biomed. Eng.*, 5(0):124–131, 2016.

[5] Roman Hovorka, Valentina Canonico, Ludovic J Chassin, Ulrich Haueter, Massimo Massi-Benedetti, Marco Orsini Federici, Thomas R Pieber, Helga C Schaller, Lukas Schaupp, Thomas Vering, and Malgorzata E Wilinska. Nonlinear model predictive control of glucose concentration in subjects with type 1 diabetes. *Physiol. Meas.*, 25(4):905–920, August 2004.

[6] Ngo P. & Tejedor M. & Tayefi M. & Chomutare T. & Godtliebsen F. Risk-averse food recommendation using bayesian feedforward neural networks for patients with type 1 diabetes doing physical activities. pages Page 1–13, 2020.

[7] Chiara Dalla Man, Francesco Micheletto, Dayu Lv, Marc Breton, Boris Kovatchev, and Claudio Cobelli. The UVA/PADOVA type 1 diabetes simulator: New features. *J. Diabetes Sci. Technol.*, 8(1):26–34, January 2014.

[8] World Health Organization diabetes. `https://www.who.int/health-topics/diabetes#tab=tab_1`. Accessed: December 18, 2023.

[9] Tejedor M. Glucose regulation for in-silico type 1 diabetes patients using reinforcement learning. 2021.

[10] David M. Nathan. Long-term complications of diabetes mellitus. *New England Journal of Medicine*, 328(23):1676–1685, June 1993.

[11] UVA Health type 1 vs type 2 diabetes. https://uvahealth.com/services/diabetes-care/types. Accessed: August 4, 2024.

[12] World Health Organization diabetes. https://www.who.int/health-topics/diabetes#tab=tab_1. Accessed: August 4, 2024.

[13] National Institut of Health gestational diabetes. https://www.niddk.nih.gov/health-information/diabetes/overview/what-is-diabetes/gestational. Accessed: August 4, 2024.

[14] Pia V Röder, Bingbing Wu, Yixian Liu, and Weiping Han. Pancreatic regulation of glucose homeostasis. *Exp. Mol. Med.*, 48(3):e219, March 2016.

[15] Varges E. & Carrillo Sepuveda MA. *Biochemistry, Insulin Metabolic Effects*. StatPearls Publishing LLC, StatPearls [Internet], September 2022.

[16] Bergmann NC Rix I, Nexøe-Larsen C. Glucagon physiology. Availeble: https://www.ncbi.nlm.nih.gov/books/NBK279127/, 2019. Accessed: August 6, 2024.

[17] Martin A Holesh JE, Aslam S. Physiology, carbohydrates. Availeble: https://www.ncbi.nlm.nih.gov/books/NBK459280/#:~:text=Carbohydrate%20digestion%20begins%20in%20the,the%20pancreas%20to%20secrete%20insulin., 2019. Accessed: August 6, 2024.

[18] Marc D. Breton. Physical activity—the major unaccounted impediment to closed loop control. *Journal of Diabetes Science and Technology*, 2(1):169–174, January 2008.

[19] Diabetes UK differences between type 1 and type 2 diabetes. https://www.diabetes.org.uk/diabetes-the-basics/differences-between-type-1-and-type-2-diabetes. Accessed: August 11, 2024.

[20] Diabetes UK insulin overdose (accidental). https://www.diabetes.org.uk/guide-to-diabetes/managing-your-diabetes/treating-your-diabetes/insulin/insulin/accidental-overdose#:~:text=What%20to%

20do%20if%20you,could%20even%20lead%20to%20death. Accessed: September 11, 2024.

[21] Diabetes.co.uk basal bolus injection regimen. https://www.diabetes.co.uk/insulin/basal-bolus.html#:~:text=A%20basal%2Dbolus%20routine%20involves,glucose%20levels%20resulting%20from%20meals. Accessed: August 11, 2024.

[22] H. S. Buholdt. Comparing reinforcement learning and traditional methods for blood glucose control in in-silico type-1 diabetes patients. pages 1–28, 2024.

[23] Günther Schmelzeisen-Redeker, Michael Schoemaker, Harald Kirchsteiger, Guido Freckmann, Lutz Heinemann, and Luigi Del Re. Time delay of CGM sensors: Relevance, causes, and countermeasures. *J. Diabetes Sci. Technol.*, 9(5):1006–1015, August 2015.

[24] Ghazanfar H. & Rizvi S.W. & Khurram A. & Orooj F. & Qaiser I. Impact of insulin pump on quality of life of diabetic patients. *Indian Journal of Endocrinology and Metabolism*, pages 506–11, 2016.

[25] Terry G Farmer, Jr, Thomas F Edgar, and Nicholas A Peppas. The future of open- and closed-loop insulin delivery systems. *J. Pharm. Pharmacol.*, 60(1):1–13, January 2008.

[26] Sasan Adibi, editor. *Mobile health; A technology road map*. Springer Series in Bio-/Neuroinformatics. Springer International Publishing, January 2015.

[27] Chirath Hettiarachchi, Elena Daskalaki, Jane Desborough, Christopher J Nolan, David O'Neal, and Hanna Suominen. Integrating multiple inputs into an artificial pancreas system: Narrative literature review. *JMIR Diabetes*, 7(1):e28861, February 2022.

[28] D J Jenkins, T M Wolever, R H Taylor, H Barker, H Fielden, J M Baldwin, A C Bowling, H C Newman, A L Jenkins, and D V Goff. Glycemic index of foods: a physiological basis for carbohydrate exchange. *Am. J. Clin. Nutr.*, 34(3):362–366, March 1981.

[29] Dionysios Vlachos, Sofia Malisova, Fedon A Lindberg, and Georgia Karaniki. Glycemic index (GI) or glycemic load (GL) and dietary interventions for optimizing postprandial hyperglycemia in patients with T2 diabetes: A review. *Nutrients*, 12(6):1561, May 2020.

[30] Amin Esfahani, Julia M W Wong, Arash Mirrahimi, Korbua Srichaikul,

David J A Jenkins, and Cyril W C Kendall. The glycemic index: Physiological significance. *J. Am. Coll. Nutr.*, 28(sup4):439S–445S, August 2009.

[31] Ashenafi Zebene Woldaregay, Eirik Årsand, Ståle Walderhaug, David Albers, Lena Mamykina, Taxiarchis Botsis, and Gunnar Hartvigsen. Data-driven modeling and prediction of blood glucose dynamics: Machine learning applications in type 1 diabetes. *Artif. Intell. Med.*, 98:109–134, July 2019.

[32] Rocio Rivas, Edward Dratz, Thomas Wagner, Gary Secor, Amanda Leckband, and David C Sands. Rapid screening of sixty potato cultivars for starch profiles to address a consumer glycemic dilemma. *PLoS One*, 18(5):e0255764, May 2023.

[33] Food and Agriculture Organization of the United Nations. *Carbohydrates in Human Nutrition*. Food & Agriculture Organization of the United Nations (FAO), Rome, Italy, July 1998.

[34] Jennie C Brand-Miller, Karola Stockmann, Fiona Atkinson, Peter Petocz, and Gareth Denyer. Glycemic index, postprandial glycemia, and the shape of the curve in healthy subjects: analysis of a database of more than 1,000 foods. *Am. J. Clin. Nutr.*, 89(1):97–105, January 2009.

[35] Fiona S Atkinson, Kaye Foster-Powell, and Jennie C Brand-Miller. International tables of glycemic index and glycemic load values: 2008. *Diabetes Care*, 31(12):2281–2283, December 2008.

[36] Chiara Dalla Man, Robert A Rizza, and Claudio Cobelli. Meal simulation model of the glucose-insulin system. *IEEE Trans. Biomed. Eng.*, 54(10):1740–1749, October 2007.

[37] Richard N Bergman. Toward physiological understanding of glucose tolerance: Minimal-model approach. *Diabetes*, 38(12):1512–1527, December 1989.

[38] Pasquale Palumbo, Susanne Ditlevsen, Alessandro Bertuzzi, and Andrea De Gaetano. Mathematical modeling of the glucose-insulin system: a review. *Math. Biosci.*, 244(2):69–81, August 2013.

[39] Roberto Visentin. In silico testing of artificial pancreas and new type 1 diabetes treatments: Model development and assessment. 2016.

[40] Xie J. Simglucose. Available: `https://github.com/jxx123/simglucose`,

2018. Accessed: December 18, 2023.

[41] Towers M & Terry J.K. & Kwiatkowski A. & Balis J.U. & de Cola G. & Deleu T.& Goulão M. & Kallinteris A. & KG A. & Krimmel M. & Perez-Vicente R. & Pierré A. & Schulhoff S. & Tai J.J. & Tan A.J.S. & Younis O.G. Gymnasium. Accessed: December 18, 2023.

[42] Mehrad Jaloli and Marzia Cescon. Modeling physical activity impact on glucose dynamics in people with type 1 diabetes for a fully automated artificial pancreas. 2023.

[43] T Nowicki. Virtual therapy using type 1 diabetes direct simulator. *J. Phys. Conf. Ser.*, 1736(1):012031, January 2021.

[44] C.D. Man, M. Camilleri, and C. Cobelli. A system model of oral glucose absorption: Validation on gold standard data. *IEEE Transactions on Biomedical Engineering*, 53(12):2472–2478, December 2006.

[45] Christian Salomonsen. Uncertainty guided polygon generation for building detection. 2024.

[46] K. Koutroumbas and S. Theodoridis. *Pattern Recognition*. Academic Press, Burlington, San Diego, London, 4 edition, 2009.

[47] Marzieh Hasannasab, Johannes Hertrich, Sebastian Neumayer, Gerlind Plonka, Simon Setzer, and Gabriele Steidl. Parseval proximal neural networks. *J. Fourier Anal. Appl.*, 26(4), August 2020.

[48] MedlinePlus glucose tolerance test - non-pregnant. `https://medlineplus.gov/ency/article/003466.htm`. Accessed: November 22, 2024.

[49] Breton M. D. Cobelli C. Man C. D. Kovatchev, B. P. Method, system and computer simulation environment for testing of monitoring and control strategies in diabetes, January 28 2020. US 10,546,659 B2.

[50] Patricio Colmegna, Ke Wang, Jose Garcia-Tirado, and Marc D Breton. Mapping data to virtual patients in type 1 diabetes. *Control Eng. Pract.*, 103(104605):104605, October 2020.

[51] Steven T Devor. Resting heart rate. *Central Ohio Primary Care: Upper Arlington Preventative Primary Care*.

[52] S M Fox, 3rd, J P Naughton, and W L Haskell. Physical activity and the prevention of coronary heart disease. *Ann. Clin. Res.*, 3(6):404–432,

December 1971.

A

Appendix

A.1 Code

The code and patient parameters used for the proposed GI extension presented in the thesis can be found at:
`https://github.com/HavardStridBuholdt/Code_for_FYS3941.git`.

The proposed extension was implemented on Xie's *simglucose* [40], the open source version of the UVA/Padova simulator. In addition to the modifications described in part II, were adjustments made to the meal announcement, simulation scenarios and environment to comply with the changes. The description of the pre-planed meals was extended to allow user to specify consumption time, carbohydrate content and GI of each simulated meal. And Jaloli's PA extension was added to allow user specified exercise sessions to be simulated.